Resonance-Tunneling Spectroscopy of Atoms Adsorbed on Metal Surfaces: Theory

J. W. GADZUK
National Bureau of Standards, Washington, D. C. 20234
(Received 13 June 1969)

Using a perturbational approach, we consider the theory of resonance tunneling of field-emitted electrons through atoms adsorbed on metal surfaces, first treated by Duke and Alferieff. It is shown how one can proceed from the observed total energy distributions to information concerning the energy-level spectrum of the atom perturbed by the metal surface. The major alteration of the spectrum manifests itself in a shift and lifetime broadening of the atomic energy levels due to configuration interactions with the continuum of metal states. In past work, this shift and broadening have been theoretically calculated by various workers. Theories have also been advanced for calculating dipole moments and, consequently, work-function changes and binding energies in which the final expressions for these quantities require knowledge of the perturbed atomic energy-level scheme. The plan in the present paper is to present a method of analyzing the data obtained in resonance-tunneling spectroscopy so that values for the shift and broadening of the energy levels can be obtained. To proceed towards this end, a simplified model is treated in a mathematically systematic manner. We believe, however, that the present approach maintains sufficiently close contact with the physics of the processes involved and thus, because of its transparency, is a potentially more valuable tool than past theories. The first experimental data of resonance tunneling in field emission, obtained by Plummer and Young and reported on in the preceding paper, are analyzed within the context of the present theory. These data include tunneling through single Zr atoms in which a single broad ground-state level is seen, tunneling through Ba atoms in which both a broad ground state of $6s^2$ character and two narrow excited $6s\ 5d$ states are seen, and tunneling through Ca in which a somewhat narrow $4s\ 4p$ excited state is seen. Most aspects of the data are satisfactorily accounted for in the present theory, and the observed shifts and broadenings of the levels are in good agreement with past calculations.

I. INTRODUCTION

THE importance of resonance tunneling of field-emitted electrons from metals upon which atoms are adsorbed has recently been pointed out by Duke and Alferieff[1] (DA). Resonance effects should be observable as structure in the total energy distribution (TED)[2] of field-emitted electrons reflecting the perturbed energy levels of the adsorbed atom. The generally accepted picture of electropositive atom adsorption is as follows. An atom is brought into contact with the metal as

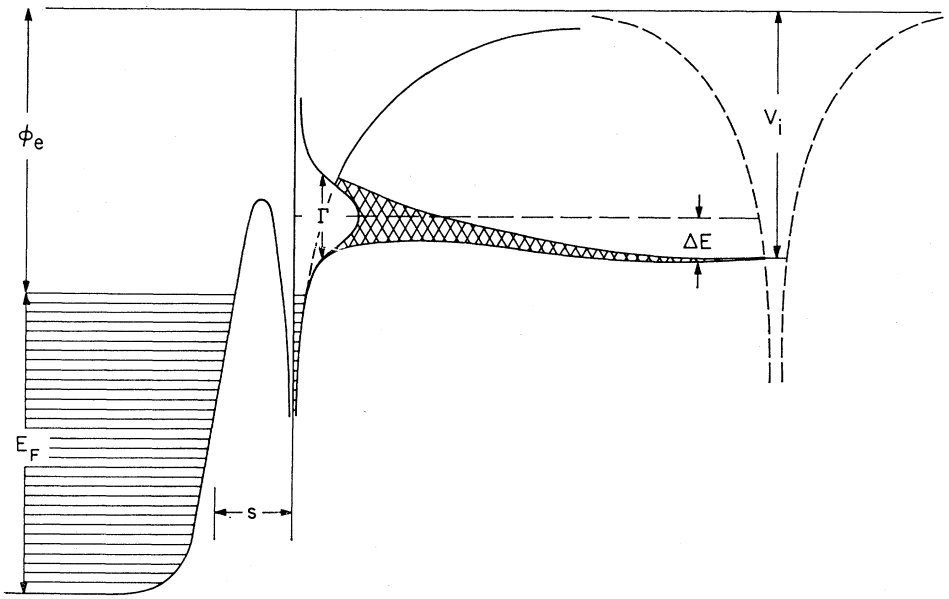

FIG. 1. Energy-level diagram relevant to a metal-surface impurity problem. The dashed curve is the ion-core potential for the particle at infinity. The solid curve is a schematic of the combined atomic and metal potential for the atom a distance s from the surface. The details of the potential between the atom and metal are only qualitatively depicted here. V_i represents the ionization energy of the isolated atom, ΔE is the shift of the energy level, and Γ is the natural broadening due to the atom's interaction with the solid. The "tornadolike" structure depicts this graphically.

[1] C. B. Duke and M. E. Alferieff, J. Chem. Phys. **46**, 923 (1967).
[2] R. D. Young, Phys. Rev. **113**, 110 (1959).

shown in Fig. 1. The originally unperturbed ground-state level is shifted and broadened into a virtual state due to a configuration interaction with the continuum of metallic states.[3–12] The situation is quite analogous to the formation of localized real and virtual impurity states in the solid.[13–15] A major aim in theoretical treatments of the atom-metal interaction at the surface has been calculation of the parameters characterizing the atom-metal interaction, namely, the energy shift ΔE and the level width Γ.[4–7] Knowing the values of ΔE and Γ, it is then possible to calculate the effective charge on the adatom,[5] the dipole moment of the atom-metal complex,[11] and the atomic binding energy.[7,10,12] Hence, an experimental means of observing the perturbed atomic energy-level scheme is desirable. Previously, these quantities have been experimentally accessible only through the ion neutralization experiments of Hagstrum and co-workers.[16] However, difficulties in the unfolding of the observed transition densities limit the ease and reliability of an accurate determination of ΔE and Γ.[17]

DA, in what is perhaps one of the most significant recent advances in surface physics, realized that in fact some manifestation of the line shapes of the perturbed atom spectra could be observed in tunneling experiments.[1] In field-emission experiments, as shown in Fig. 2(a), the TED of emitted electrons is given by an expression of the form $dj_0/dE=(J_0/d)e^{E/d}$ at zero temperature for energies below the Fermi level with J_0 equal to some constant and $1/d=0.51\varphi^{1/2}/F$ eV^{-1} where φ is the electron work function in eV, E is electron energy, and F is the applied field in V/Å. Typically, 0.1 eV$\lesssim d\lesssim$0.2 eV in field-emission experiments. However, in the presence of an adsorbed atom with a narrow energy level lying within the energy range measured, resonance tunneling can occur, giving rise to the idealized TED shown in Fig. 2(b). If the energy of the tunneling electron lies within an energy level of the atom, the electron can tunnel into the atom, get across the spatial domain of the atom without any decrease in probability amplitude, and then tunnel through the considerably narrower barrier as shown in Fig. 3. (Figure 3 is not drawn to scale. In actuality $s\approx 3$ Å, whereas $s_T\approx 20$ Å.) Also shown schematically are electron wave functions for the metal, virtual atomic, and free states. The direct-tunneling amplitude is proportional to the overlap of $|m\rangle$, the metal wave function, and $|f\rangle$, the free function, whereas the resonance tunneling is proportional to the overlap of $|m\rangle$ and $|a\rangle$ times the overlap of $|f\rangle$ and $|a\rangle$, where $|a\rangle$ is the virtual atomic-state wave function. In Fig. 3, the atomic potential is represented by a square well of an appropriate depth and width to be the "right size" for the atom and also to produce bound states at the proper energy. DA characterize resonance tunneling by an enhancement factor

$$R(E)\equiv \frac{dj}{dE}\Big/\frac{dj_0}{dE},$$

where dj/dE is the TED in the presence of the atom. Comparing the schematic TED's in Figs. 2(a) and 2(b), it is seen that structure will then appear in $R(E)$ which should in some way reflect the virtual atomic state. We should point out, however, that both j' and j_0' must be corrected for area effects since the probe hole through which the field-emission current is measured sees an area of about 25 surface atoms.[18] The addition of a single adsorbate atom will affect the TED only within the limits of an appropriate area ratio factor.[19] The maximum in the enhancement factor for emission through the impurity can be very large, falling within the range $1<R(E)\lesssim 10^4$.

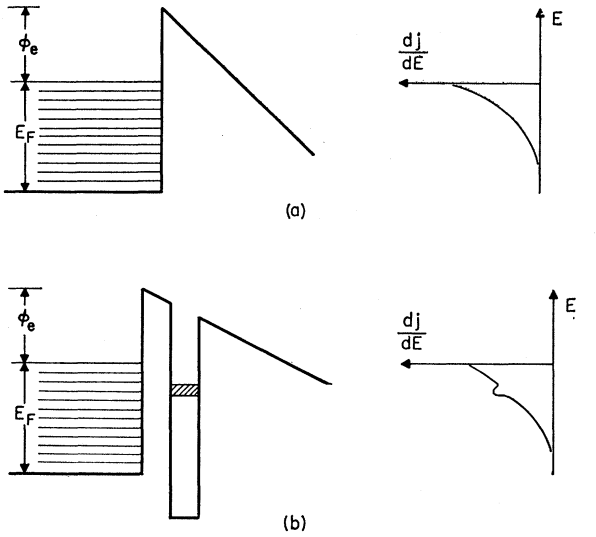

FIG. 2. (a) Model potential and total energy distribution for field emission from a metal. (b) Model potential and total energy distribution for resonance-tunneling field emission from a metal with a narrow-band adsorbate.

[3] U. Fano, Phys. Rev. **124**, 1866 (1961).
[4] R. Gomer and L. W. Swanson, J. Chem. Phys. **38**, 1613 (1963).
[5] A. J. Bennett and L. M. Falicov, Phys. Rev. **151**, 512 (1966).
[6] J. W. Gadzuk, Surface Sci. **6**, 133 (1967).
[7] L. Schmidt and R. Gomer, J. Chem. Phys. **45**, 1605 (1966).
[8] T. B. Grimley, Proc. Phys. Soc. (London) **90**, 751 (1967).
[9] D. M. Edwards and D. M. Newns, Phys. Letters **24A**, 236 (1967).
[10] D. M. Newns, Phys. Rev. **178**, 1123 (1969).
[11] J. W. Gadzuk, in *The Structure and Chemistry of Solid Surfaces*, edited by G. A. Somorjai (John Wiley & Sons, Inc., New York, 1969).
[12] K. Hartman, J. W. Gadzuk, and T. N. Rhodin (unpublished).
[13] G. F. Koster and J. C. Slater, Phys. Rev. **95**, 1167 (1954); **96**, 1208 (1954).
[14] P. W. Anderson, Phys. Rev. **124**, 41 (1961).
[15] A. M. Clogston, Phys. Rev. **125**, 439 (1962).
[16] H. D. Hagstrum and G. E. Becker, Report on Twenty-seventh Physical Electronics Conference, MIT, Cambridge, Mass., 1967, p. 122 (unpublished); and Ref. 11.
[17] H. D. Hagstrum, Phys. Rev. **150**, 495 (1966).
[18] E. W. Müller, J. Appl. Phys. **26**, 732 (1955).
[19] E. W. Plummer and T. N. Rhodin, Appl. Phys. Letters **11**, 194 (1967).

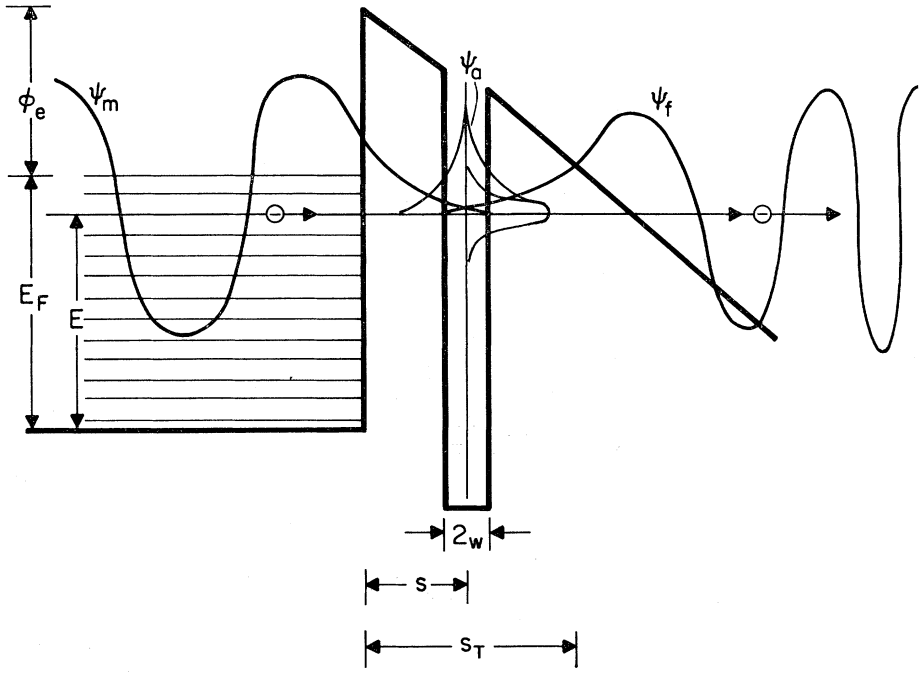

FIG. 3. Schematic model showing the idealized potentials relevant in resonance tunneling. The electron wave functions are: ψ_m, the unperturbed metal function; ψ_a, the localized virtual impurity function; and ψ_f, the emitted electron function which will be used in subsequent calculations.

DA chose to exhibit the resonance-tunneling effect by adopting a model first used by Ioganson.[20] In this model DA use idealized potentials such as those shown in Fig. 3 and do an exact evaluation, through a matching-wave-functions technique, of the transmission coefficient with and without the atom. The atomic potential is represented both by a square-well attractive core and repulsive δ-function pseudopotential performing the role of orthogonalization to core states. However, it is hard to generalize their model calculation to more realistic systems, and because of the numerical nature of their final results it is difficult to go from the shape of the $R(E)$ curve to a statement of the values of the energy-level parameters ΔE and Γ.

Since the goal of the present work is to show how the measured $R(E)$ curves can be analyzed to obtain values for ΔE and Γ, we chose to reformulate the theory of resonance tunneling in a much different manner, making closer identification with the concepts and notation of past work on surface-impurity virtual states.[4–11] A theory which is a hybridization of the Oppenheimer perturbation theory,[21] rearrangement collision theory,[22] configuration-interaction theory,[3] WKB tunneling theory,[23] and surface-impurity theory[4–10] is presented here. The end result of the calculations, a current-enhancement factor $R(E)$, is given as a function of the previously mentioned quantities ΔE and Γ plus other system parameters and tunneling matrix elements or tunneling probabilities. Preliminary versions of the theory have been successfully used to interpret experimental resonance-tunneling currents through Zr atoms[24] and Ba atoms.[25] The effects of multilevel atoms and excited states of the atom are displayed. Comparison between theory and the experimental reuslts of Plummer and Young, given in the preceding paper,[26] are made or, alternatively, the experimental results are analyzed within the context of the present theory. Of major interest is the work pertaining to Ba on tungsten. In this system a true energy spectrum is seen which we believe to be some manifestation of a $6s^2$ ground state, a $6s5d$ triplet excited state, and a $6s5d$ singlet excited state. The observed resonance-tunneling spectrum is in good agreement with theoretical calculations, a fact which we think lends support to the validity of the theoretical picture outlined here. The relative computational ease in which theoretical enhancement factors are calculated also makes the present theory potentially useful and attractive for analyzing future resonance-tunneling spectra.

The structure of the paper is as follows. In Sec. II, the general philosophy of the theory is put forth. The relationship between the atomic level parameters ΔE and Γ and other aspects of the resonance-tunneling

[20] L. V. Iogansen, Zh. Eksperim. i Teor. Fiz. **45**, 207 (1963); **47**, 270 (1964) [English transls.: Soviet Phys.—JETP **18**, 146 (1964); **20**, 180 (1965)].
[21] J. R. Oppenheimer, Phys. Rev. **31**, 66 (1928).
[22] T. Y. Wu and T. Ohmura, *Quantum Theory of Scattering* (Prentice-Hall, Inc., Englewood Cliffs, N. J., 1962), p. 211.
[23] E. Merzbacher, *Quantum Mechanics* (John Wilev & Sons, Inc., New York, 1961), p. 112.
[24] E. W. Plummer, J. W. Gadzuk, and R. D. Young, Solid State Commun. **7**, 487 (1969).
[25] J. W. Gadzuk, E. W. Plummer, and R. D. Young, Bull. Am. Phys. Soc. **11**, 399 (1969).
[26] E. W. Plummer and R. D. Young, preceding paper, Phys. Rev. B **1**, 2088 (1970).

phenomenon is established. General formulas for the current-enhancement factor are obtained in terms of various matrix elements. The effects of two-electron excited states are considered. Section III is basically a technical section devoted to the calculation of the required matrix elements. In Sec. IV, the numerical results appear. Here the experimental $R(E)$ curves are analyzed in terms of the theory of Secs. II and III and assignments are made for the values of ΔE and Γ. Cases considered are Zr, Ba, and Ca on tungsten. Section V is devoted to general conclusions and discussion.

II. RESONANCE-TUNNELING THEORY

There exist in the literature, various theoretical studies treating different aspects of field emission from perfect free-electron metals,[2,27,28] metals with band structures,[29–31] arbitrary metals,[32] and superconductors,[32–34] mostly from a WKB point of view. Theoretical workers in normal metal and superconductor junction tunneling have framed the problem of tunneling within a Hamiltonian point of view.[35–39] In these treatments, the full Hamiltonian of the system is divided into three parts, the first and second being the unperturbed Hamiltonians of the left- and right-hand sides of the junction if the other side was not present and the third being what is called the tunneling Hamiltonian, the operator which allows each side to know of the other side's existence and thus measures the rate of tunneling. Essentially this operator is the matrix element or overlap integral of the exponentially damped tails of the left- and right-hand-side states with some appropriate barrier potential. Often this matrix element is evaluated within the WKB or effective-mass approximation.[40] This procedure is reasonably easy to carry out provided the problem can be reduced to an effective one-dimensional problem and the form of the junction barriers is simple. However, this approach is limited when one considers three-dimensional systems or tunneling which involves various angular momentum states of atoms.

In the past, it has been customarily accepted that tunneling effects of electrons between metals and virtual atomic states associated with adsorbed atoms could be satisfactorily considered within the context of the Oppenheimer field-ionization approximation.[4–7,16,17,21] In the original work of Oppenheimer, the field ionization of an isolated hydrogen atom was considered as shown in Fig. 4. A strong electric field was applied to the atom, reducing the potential barrier on one side thus making tunneling from the atomic state to a free Airy-function state possible. The tunneling was viewed as a transition from an atomic to free state induced by the perturbation of the applied field. The dynamics were then handled through time-dependent perturbation theory in which the transition probability was characterized by a matrix element $T=\langle \text{free}|eFz|\text{atom}\rangle$ in which $|\text{atom}\rangle$ is the atomic wave function, $|\text{free}\rangle$ is the Airy function, and F is the applied field in the z direction. This approach has been discussed further by Lanczos.[41] In many senses, this manner of thinking is formally equivalent to configuration interactions between the bound atomic configuration and the free continuum configuration at the same energy.[3] There is also a formal similarity between this type of approach and that used in rearrangement collisions between states of different unperturbed initial and final Hamiltonians.[22,31,42] Although there exist some manageable mathematical difficulties due to the fact that one deals with transitions between nonorthogonal states, some of these problems can be dealt with by properly orthogonalizing the initial and final states.[38,42,43] In spite of

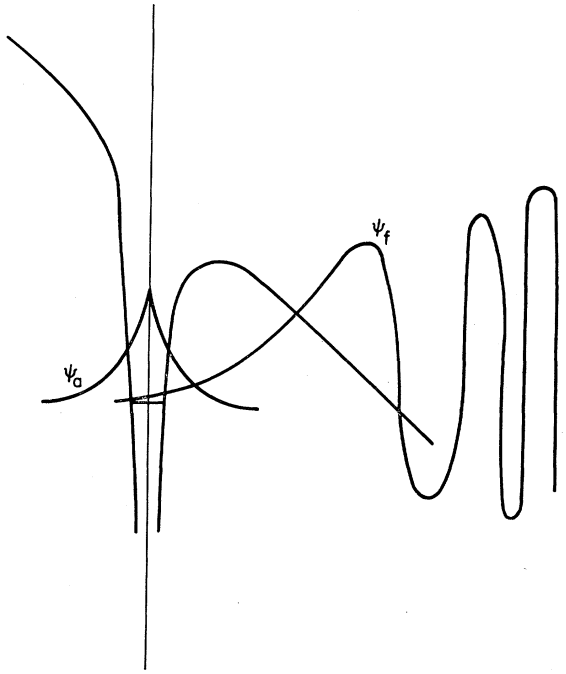

FIG. 4. The potentials and electron wave functions for field ionization of hydrogen atoms treated by Oppenheimer.

[27] L. W. Nordheim, Proc. Roy. Soc. (London) **A121**, 626 (1928).
[28] R. H. Fowler and L. W. Nordheim, Proc. Roy. Soc. (London) **A119**, 173 (1928).
[29] R. Stratton, Phys. Rev. **135**, A794 (1964).
[30] F. I. Itskovich, Zh. Eksperim. i Teor. Fiz. **50**, 1425 (1966); **52**, 1720 (1967) [English transls.: Soviet Phys.—JETP **23**, 945 (1966); **25**, 1143 (1967)].
[31] J. W. Gadzuk, Phys. Rev. **182**, 416 (1969).
[32] J. W. Gadzuk, Surface Sci. **15**, 466 (1969).
[33] G. A. Gogadze and I. O. Kulik, Fiz. Metal. Metalloved. **23**, 606 (1967).
[34] A. Leger, J. Phys. (Paris) **29**, 646 (1968).
[35] W. A. Harrison, Phys. Rev. **123**, 85 (1961).
[36] J. Bardeen, Phys. Rev. Letters **6**, 502 (1961).
[37] M. H. Cohen, L. M. Falicov, and J. C. Phillips, Phys. Rev. Letters **8**, 316 (1962).
[38] R. E. Prange, Phys. Rev. **131**, 1083 (1963).
[39] V. Ambegaokar and A. Baratoff, Phys. Rev. Letters **10**, 486 (1963).
[40] D. J. BenDaniel and C. B. Duke, Phys. Rev. **152**, 683 (1966).
[41] C. Lanczos, Z. Physik **68**, 204 (1931).
[42] J. W. Gadzuk, Surface Sci. **6**, 159 (1967).
[43] M. H. Mittleman, Phys. Rev. **122**, 1930 (1961).

these formal problems, the Oppenheimer approach has proven useful and has provided results in surface-impurity theories which are in quite good agreement with experimental results.[5,6,24–26] Another virtue of the approach is that it enables one to calculate relative transition or tunneling probabilities between atomic states of various angular momentum quantum numbers and other relative transition probabilities.

The general philosophy to be used in this paper is as follows. We will view field emission from metals in a manner similar to Oppenheimer field ionization of atoms. Whenever we require relative tunneling probabilities or the ratio of two different probabilities, we will obtain this ratio by taking ratios of Oppenheimer probabilities. However, when we need absolute values of tunneling probabilities we will use the more widely accepted WKB results. For example, in the present scheme the tunneling probability from, say, a d level would be given by $\{P_{\mathrm{Opp}}{}^d/P_{\mathrm{Opp}}{}^s\}P_{\mathrm{WKB}}{}^s$ where the subscript Opp means the probability evaluated within the Oppenheimer scheme. In this way we hope to capture some of the influences of various atomic states in our theory which could not be treated in a standard WKB way.

The first item is to consider normal-field emission as shown in Fig. 2(a). Here the full single-electron Hamiltonian is written as

$$\begin{aligned} H&=\mathrm{KE}+V_m+V_{\mathrm{F}} \\ &=H_0{}^m+V_{\mathrm{F}}=H_0{}^f+V_m, \end{aligned} \tag{1}$$

where KE is the kinetic-energy operator, V_m, the potential of the metal, equals 0 for $z<0$, equals $E_{\mathrm{F}}+\varphi_e$ for $z\geq 0$ with E_{F} equal to the Fermi energy and φ_e equal to the electron work function and $V_F=eFz$, the potential of the applied field. From Eq. (1) we can identify two sets of states, the first being eigenfunctions of the metal $H_0{}^m|m\rangle=\mathcal{E}_m|m\rangle$ and the second being eigenfunctions of the applied-field potential $H_0{}^f|f\rangle=\mathcal{E}_f|f\rangle$. Within the Oppenheimer scheme, tunneling from the metal to the free states would be characterized by a matrix element

$$T_0=\langle f|V_F|m\rangle. \tag{2}$$

We next suppose that an atom is adsorbed on the metal surface, thus providing an additional term in the Hamiltonian, the atomic potential as seen in Fig. 2(b). Furthermore, the presence of the atom will induce screening or polarization charge in the metal, possibly changing the form of V_m slightly.[44] The new Hamiltonian will then appear as

$$H=\mathrm{KE}+V_m{}'+V_a+V_F, \tag{3}$$

where $V_m{}'$ is the new metal potential and V_a is the atomic-core potential. We now introduce another set of states, the unperturbed atomic eigenfunctions through $H_0{}^a|a_0\rangle=(\mathrm{KE}+V_a)|a_0\rangle=\mathcal{E}_a{}^0|a_0\rangle$. If we consider the part of the full Hamiltonian, Eq. (3),

$$H_0{}^{a-m}=\mathrm{KE}+V_m{}'+V_a, \tag{4}$$

it is seen that this is the same Hamiltonian used in past work on virtual surface-impurity states.[4–7] In these works it was shown that an electron in an unperturbed atomic state will experience an energy shift $\Delta E=\langle a_0|V_m{}'|a_0\rangle$ and a lifetime broadening

$$\Gamma=2\pi\textstyle\sum_m \delta(E-E_m)|\langle m|V_m{}'|a_0\rangle|^2$$

due to the configuration interaction of the discrete atomic state with the continuum of metallic states. The atomic state is mixed with metal states and in first-order perturbation theory, the new atomic state satisfying

$$(\mathrm{KE}+V_m{}'+V_a)|a\rangle=\mathcal{E}_a{}'|a\rangle \tag{5}$$

is given by

$$|a\rangle=|a_0\rangle+\sum_m \frac{|m\rangle\langle m|V_m{}'|a_0\rangle}{E-E_m}. \tag{6}$$

Although one might question the validity of using such a perturbational approach in which mixing between the impurity and continuum states is treated only in lowest order, we should note that this approximation is entirely equivalent to using the Anderson Hamiltonian in the single-electron approximation.[5,6,10,14] This is discussed at greater length in the Appendix. We feel that since an adsorbed atom is more isolated from the host metal than an impurity of the Anderson type, it certainly is a reasonable first approximation to use the weak-coupling theory for bulk impurities to describe the even weaker-coupling case of a surface impurity. Another check on the validity of our procedure is related to the magnitude of the imaginary part of the virtual-impurity-state energy. If this lifetime broadening is much less than the width of the metal conduction band, then the simple mixing given by Eq. (6) is an adequate first approximation. From past work we know that this is the case; the atomic energy level for an s state acquires a lifetime width of about 1 eV as contrasted with a conduction-band width of more than 10 eV. Thus the Anderson virtual-impurity-state theory seems to be a reasonably justified way of looking at the problem.

The full Hamiltonian of Eq. (3) is now written as

$$H=H_0{}^{a-m}+V_F. \tag{7}$$

To consider the possibilities of resonance tunneling due to an intermediate state in which the tunneling electron sits at the atom-core site, write the Oppenheimer tunneling matrix element, Eq. (2), one higher order in perturbation theory with the Hamiltonian divided as in Eq. (7). Thus

$$T=\langle f|V_f+V_F(E-H_0{}^{a-m})^{-1}V_F|m\rangle. \tag{8}$$

[44] J. W. Gadzuk, Solid State Commun. 5, 743 (1967).

For illustrative purposes first assume that we are dealing with a single-level atom perturbed by the metal potential. Also assume that the metal, atom, and free states are orthogonal. Then we can insert the "complete set" of intermediate perturbed atomic states given by Eq. (6) into Eq. (7) with the result that

$$(E-H_0{}^{a-m})^{-1}\rightarrow|a\rangle(E-\mathcal{E}_a{}')^{-1}\langle a|\,. \tag{9}$$

At this point we need an explicit expression for $\mathcal{E}_a{}'$ given by Eq. (5) as $\mathcal{E}_a{}'=\langle a|\mathrm{KE}+V_a+V_m{}'|a\rangle$. Using the perturbed atomic states, Eq. (6), we get

$$\begin{aligned}\mathcal{E}_a{}'=&\langle a_0|H_0{}^a+V_m{}'|a_0\rangle\\&+\sum_m\frac{\langle a_0|H_0{}^a+V_m{}'|m\rangle\langle m|V_m{}'|a_0\rangle}{E-E_m}\\&+\sum_m\frac{\langle m|H_0{}^a+V_m{}'|a_0\rangle\langle a_0|V_m{}'|m\rangle}{E-E_m}\\&+\sum_{m,m'}\frac{\langle m'|H_0{}^a+V_m{}'|m\rangle\langle m|V_m{}'|a_0\rangle\langle a_0|V_m{}'|m'\rangle}{(E-E_m)(E-E_m{}')}.\end{aligned}$$

The first matrix element is simply $\langle a_0|H_0{}^a+V_m{}'|a_0\rangle=\mathcal{E}_a{}^0+\langle a_0|V_m{}'|a_0\rangle=\mathcal{E}_a{}^0+\Delta E$, where $\mathcal{E}_a{}^0$ is the unperturbed eigenvalue and ΔE is the first-order shift calculated previously.[6] The last term is a small correction to ΔE which can be handled using a procedure established by Fano.[3] The matrix elements in the second and third term are $\langle a_0|H_0{}^a+V_m{}'|m\rangle=\mathcal{E}_a{}^0\langle a_0|m\rangle+\langle a_0|V_m{}'|m\rangle=\langle a_0|V_m{}'|m\rangle$ owing to the assumed orthogonality, $\langle a_0|m\rangle=0$. Thus

$$\mathcal{E}_a{}'=\mathcal{E}_a{}^0+\Delta E+2\sum_m\frac{|\langle m|V_m{}'|a_0\rangle|^2}{E-E_m}.$$

Now if we take $(E-E_m)^{-1}=P(E-E_m)^{-1}+i\pi\delta(E-E_m)$ with P a principle-part integral which is taken to be a negligible correction to the real part of the energy, then

$$\begin{aligned}\mathcal{E}_a{}'=\mathcal{E}_a{}^0+\Delta E+i2\pi\sum_m\delta(E-E_m)|\langle m|V_m{}'|a_0\rangle|^2\\=E_\varphi+i\Gamma,\end{aligned} \tag{10}$$

where $E_\varphi\equiv\mathcal{E}_a{}^0+\Delta E$ and Γ is the natural broadening of the atomic level, also calculated previously.[5,6] Consequently, inserting Eqs. (9) and (10) into the resonant-tunneling matrix element, Eq. (8), yields

$$T=\langle f|V_F|m\rangle+\frac{\langle f|V_F|a\rangle\langle a|V_F|m\rangle}{E-E_\varphi-i\Gamma}, \tag{11}$$

which is the usual type of matrix element describing a resonance process. The resonant intermediate state is characterized by a shift in its position and a finite lifetime, or in other words, a complex energy.[45]

[45] A. Messiah, *Quantum Mechanics* (John Wiley & Sons, Inc., New York, 1962), Vol. II, p. 1006.

The current-enhancement factor in resonance tunneling is defined as the ratio

$$R(E)=\frac{dj}{dE}\Big/\frac{dj_0}{dE},$$

where j' is the TED under resonance conditions and $j_0{}'$ is the TED without the atom present. Within the Oppenheimer scheme, the TED is proportional to the square of the tunneling matrix element. Thus $j_0{}'=\gamma|T_0|^2$ and $j'=\gamma|T|^2$, where T_0 is given by Eq. (2), T by Eq. (11), and γ is an unspecified grouping of constants and densities of final states which need not be considered here since we are taking only the ratios of tunneling probabilities consistent with our plan for using the Oppenheimer method. If we identify

$$T_a(E)=\frac{\langle f|V_f|a\rangle\langle a|V_f|m\rangle}{\langle f|V_f|m\rangle}, \tag{12}$$

then the resonance-enhancement factor assumes the form

$$\begin{aligned}R(E)=\frac{|T|^2}{|T_0|^2}=1+\frac{T_a{}^2(E)}{(E-E_\varphi)^2+\Gamma^2}\\+\frac{2(E-E_\varphi)|T_a(E)|}{(E-E_\varphi)^2+\Gamma^2}\end{aligned} \tag{13}$$

with the following interpretation. The first term on the right-hand side is just the direct-tunneling probability. The second term is the resonance-tunneling factor which is a Lorentzian reflecting the line shape of the atomic level and an energy-dependent tunneling-amplitude ratio to be discussed below. The third term is an interference term between the direct and resonance-tunneling channels. The ratio of tunneling matrix elements reflects the fact that the tunneling electron traverses the spatial domain of the atom without losing any amplitude, in effect cutting a hole out of the barrier as shown in Fig. 3. In the simplest approach for a square barrier of width s_T, the tunneling probability amplitude would be $\sim e^{-ks_T}$ with k the average propagation constant in the forbidden region. On the other hand, if a hole of width $2w$ centered at $z=s$ were cut out of the barrier, the tunneling probability amplitude would be

$$\sim\langle z=0|z=s-w\rangle\langle z=s-w|z=s+w\rangle\langle z=s+w|z=s_T\rangle,$$

where each amplitude is that to get from the left-hand limit to the right-hand one. We have $\langle 0|s-w\rangle\sim e^{-k(s-w)}$, $\langle s-w|s+w\rangle\sim 1$, and $\langle s+w|s_T\rangle=e^{-k(s_T-s-w)}$. Consequently, the resonant amplitude is $\sim e^{-k(s_T-2w)}$. The ratio of the amplitudes with and without the atom which is essentially what $T_a(E)$ is, would thus be $\sim e^{2kw}$. Hence we will expect the more detailed calculations of $T_a(E)$ to take a basically $e^{k'w}$ form with

$$k'=\tfrac{1}{2}[(2m/\hbar^2)(E_F+\varphi_e-E)]^{1/2},$$

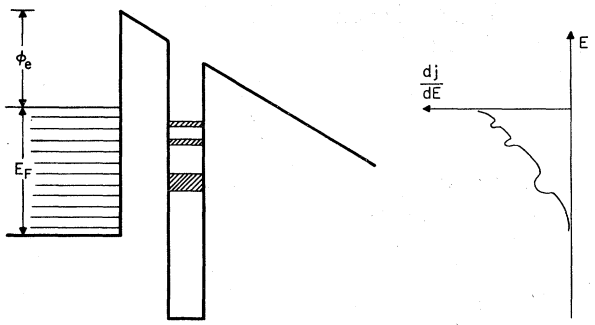

FIG. 5. Model potential and TED for resonance tunneling through a multilevel adsorbate.

the average propagation constant through a triangular barrier. This sort of simple reasoning has been successful in providing an interpretation of the preliminary Zr on tungsten resonances.[24]

The generalization of these results to the case where we consider multilevel atoms and thus excited states is simply effected by replacing Eq. (9) with

$$\frac{1}{E-H_0^{a-m}} \rightarrow \sum_i |a_i\rangle \frac{1}{E-\mathcal{E}_{a_i}'} \langle a_i| . \qquad (14)$$

Schematically the possibility of seeing excited states in a perfect experiment is shown in Fig. 5. Resonance tunneling could occur through any of the atomic virtual levels producing a true-surface-impurity virtual-energy-level diagram. It is interesting to note that Esaki, Stiles, and Chang claim to have observed atomiclike spectra of impurities in the barrier of PbTe-Al_2O_3-metal junctions very similar to the type considered here.[46] We should also note that processes other than direct elastic tunneling could occur. Inelastic processes involving phonons or localized vibrational levels probably are not too important for the cases we consider here, simple electropositive atoms on surfaces.[47] However, radiative decay, or more importantly, Auger neutralization with the subsequent production of higher-energy electrons above the Fermi level which could then tunnel could be an interesting possibility.[17] Although any Auger electrons would be small in number compared to the elastically tunneling electrons, the reduced tunneling barrier for the higher-energy Auger electrons would serve to increase their chances of being observed. This remains a question to be considered in the future.

Since one of the goals of this paper is to explain the resonance-tunneling spectra of alkaline-earth atoms and in particular Ba, we must now direct our attention to ways of handling two-electron states of adsorbed atoms. For instance, the ground state of Ba is a $6s^2$ and the two lowest excited states are $6s5d$ triplet (^3D) and $6s5d$ singlet (^1D). We will assume that to a first approximation we can take the two-electron states to be a properly symmetrized product state. Thus

$$|a_i\rangle = 2^{-1/2}[|1(\mathbf{r}_1)\rangle|2(\mathbf{r}_2)\rangle \pm |1(\mathbf{r}_2)\rangle|2(\mathbf{r}_1)\rangle], \qquad (15)$$

where each single-electron state is of the form given by Eq. (6). We view resonance tunneling involving two-electron intermediate states as a one-electron dynamical process in the following sense: Originally a singly charged ion with one outer-shell electron (or actually $Z_{\text{eff}} \leq 1$ as outlined by Bennett and Falicov depending on the level position and width relative to the Fermi level[5]) and the tunneling electron in the metal are present. The electron tunnels to the atom forming a two-electron virtual state given by Eq. (15) from which one of the electrons then tunnels to the vacuum. Exchange tunneling is allowed and treated in the formalism automatically by using properly symmetrized two-electron states. The initial state is a properly symmetrized product of a metal and atomic state, the intermediate state is of the form of Eq. (15), and the final state is also a properly symmetrized product of a free state and an atomic state. Whether the initial and final states are symmetric or antisymmetric with respect to their spatial wave functions depends upon the spin state of the intermediate state. For instance, an intermediate ^3D state requires an antisymmetric spatial function whereas the ^1D requires a symmetric spatial function. Simultaneous tunneling of both electrons is ruled out by the arguments advanced by Wilkins for pair tunneling in superconductor junctions in which two-electron processes are proportional to the square of the very small tunneling probability.[48]

Now we consider the specific case of resonance tunneling through Ba atoms. The unperturbed Ba spectrum has a $6s^2$ ground state with an antisymmetric spin state. The first excited state is the triplet $6s5d$ with a symmetric spin state, about 1.1 eV above the ground state. The second excited state is the singlet $6s5d$ with an antisymmetric spin state about 0.29 eV higher in energy.[49] We wish to consider resonance tunneling through each of these states. The first thought would be to allow for three intermediate virtual atomic states in Eq. (14). Then the tunneling matrix element, similar to Eq. (11), would contain two additional terms corresponding to the two excited states. Taking the square of T, there would result four direct tunneling terms plus 12 terms representing interferences between the various tunneling channels. However, since the ^3D state has a symmetric spin state whereas all other terms involve antisymmetric spin states, for an assumed spin-independent tunneling potential, vanishing matrix elements representing interferences of the singlet state with the ground-

[46] L. Esaki, P. J. Stiles, and L. L. Chang, Phys. Rev. Letters **20**, 1108 (1968).

[47] J. Lambe and R. C. Jaklevic, Phys. Rev. **165**, 821 (1968).

[48] J. W. Wilkins, in *Tunneling Phenomena in Solids*, edited by E. Burstein and S. Lundqvist (Plenum Press, New York, 1969), p. 333.

[49] Charlotte E. Moore, *Atomic Energy Levels*, National Bureau of Standards Publication No. 467 (U. S. Government Printing Office, Washington, D. C., 1964), Vol. I and III.

and triplet-state tunneling channels would result. Thus this particular problem of a three-level atom reduces to the sum of a two-level atom resonance plus a single-level atom resonance.

First we treat the two-level part of the problem. The initial and final two-electron states are taken as

$$|\mathrm{In}\rangle = 2^{-1/2}[|m(\mathbf{r}_1)\rangle|6s(\mathbf{r}_2)\rangle + |m(\mathbf{r}_2)\rangle|6s(\mathbf{r}_1)\rangle],$$
$$|\mathrm{Fin}\rangle = 2^{-1/2}[|f(\mathbf{r}_1)\rangle|6s(\mathbf{r}_2)\rangle + |f(\mathbf{r}_2)\rangle|6s(\mathbf{r}_1)\rangle],$$

and the intermediate states are

$$|a_0\rangle = 2^{-1/2}[|6s(\mathbf{r}_1)\rangle|6s(\mathbf{r}_2)\rangle + |6s(\mathbf{r}_2)\rangle|6s(\mathbf{r}_1)\rangle],$$
$$|a_1\rangle = 2^{-1/2}[|6s(\mathbf{r}_1)\rangle|5d(\mathbf{r}_2)\rangle + |6s(\mathbf{r}_2)\rangle|5d(\mathbf{r}_1)\rangle].$$

Taking the perturbation to be of a symmetric form $V_F = V_F(r_1) + V_F(r_2)$ and using the symmetric spatial wave functions, the resonance-tunneling matrix elements, in analogy with Eq. (11), become

$$T_{\mathrm{sym}} = \langle f|V_F|m\rangle + \frac{\langle f|V_F|6s\rangle\langle 6s|V_F|m\rangle}{E - E_\varphi^{6s} - i\Gamma_{6s}} + \frac{\langle f|V_F|5d\rangle\langle 5d|V_F|m\rangle}{E - E_\varphi^{1D} - i\Gamma^1{}_D}, \quad (16)$$

where E_φ^{6s} and E_φ^{1D} are the appropriate values of the shifted $6s^2$ and singlet $6s5d$ levels, respectively, and similarly for Γ_{6s} and $\Gamma^1{}_D$. These quantities will be calculated in subsequent sections.

The remaining excited state, the triplet $6s5d$, is handled in much the same manner except that spatially antisymmetric two-electron states are used. We then obtain

$$T_{\mathrm{anti}} = \langle f|V_F|m\rangle - \frac{\langle f|V_F|5d\rangle\langle 5d|V_F|m\rangle}{E - E_\varphi^{3D} - i\Gamma^3{}_D} \quad (17)$$

with the obvious definition for E_φ^{3D} and $\Gamma^3{}_D$. The total probability is obtained by adding the properly normalized individual probabilities such that $|T|^2 = \frac{1}{2}|T|_{\mathrm{sym}}|^2 + \frac{1}{2}|T_{\mathrm{anti}}|^2$. Each case is weighted equally since we have not bothered to distinguish between different j levels in the triplet. We do this since the resolution of the experimental apparatus was not sufficient to do so. Next we make the following identifications:

$$M_0 = \langle f|V_F|m\rangle, \quad (18a)$$
$$M_1 = \langle f|V_F|6s\rangle, \quad (18b)$$
$$M_2 = \langle 6s|V_F|m\rangle, \quad (18c)$$
$$M_3 = \langle f|V_F|5d\rangle, \quad (18d)$$
$$M_4 = \langle 5d|V_F|m\rangle. \quad (18e)$$

Then from $R(E) = |T|^2/|T_0|^2$ with T_0 given in Eq. (2) and T obtained from Eqs. (16) and (17), and using Eqs. (18a)–(18e), the current-enhancement factor is, for the three-level atom,

$$R(E) = 1 + \frac{M_1^2 M_2^2}{2M_0^2}\frac{1}{(E - E_\varphi^{6s})^2 + \Gamma_{6s}^2} + \frac{M_3^2 M_4^2}{2M_0^2}\left(\frac{1}{(E - E_\varphi^{1D})^2 + \Gamma^1{}_D{}^2} + \frac{1}{(E - E_\varphi^{3D})^2 + \Gamma^3{}_D{}^2}\right)$$
$$+ \frac{M_1 M_2}{M_0}\frac{(E - E_\varphi^{6s})}{(E - E_\varphi^{6s})^2 + \Gamma_{6s}^2} + \frac{M_3 M_4}{M_0}\left(\frac{(E - E_\varphi^{1D})}{(E - E_\varphi^{1D})^2 + \Gamma^1{}_D{}^2} - \frac{(E - E_\varphi^{3D})}{(E - E_\varphi^{3D})^2 + \Gamma^3{}_D{}^2}\right)$$
$$+ \frac{M_1 M_2 M_3 M_4}{M_0^2}\frac{[(E - E_\varphi^{6s})(E - E_\varphi^{3D}) + \Gamma_{6s}\Gamma^3{}_D]}{[(E - E_\varphi^{6s})^2 + \Gamma_{6s}^2][(E - E_\varphi^{3D}) + \Gamma^3{}_D{}^2]}. \quad (19)$$

The structure of this result is as follows. The first term represents the direct-tunneling channel. The next two terms are the three resonant-tunneling channels. The fourth and fifth terms are interference terms between the direct and three-resonance channels. The last term is an interference between the resonant $6s^2$ and $6s5d$ triplet channels. As mentioned previously, owing to spin statistics there is no interference between the $6s5d$ singlet channel and the other resonant channels. We expect the form of $R(E)$ to have a broad nonsymmetric peak representing the wide $6s^2$ state and two more narrow peaks for the two excited states. Since the triplet state interferes only with the direct channel, the shape of this peak should be similar to the single-level-atom enhancement factor such as that for Zr atoms.[24]

We have now reached the first plateau in this study of resonance tunneling, the determination of the current-enhancement factor for multilevel atoms. To proceed, the relevant matrix elements given by Eqs. (18a)–(18e) must be calculated as must the various values of E_φ and Γ. Section III deals with these rather technical details. It should be noted though that we are now finished with the present theory of resonance tunneling. The remainder of the paper is devoted to the implementation and exploitation of the theory.

III. MATRIX ELEMENTS CALCULATIONS

To proceed we now require explicit expressions for the tunneling matrix given by Eqs. (18a)–(18e) and also values for the various E_φ's and Γ's. Unfortunately, this will be a long drawn-out procedure which will not be

particularly enlightening until we get to the end results. This section is divided into four parts. Section III A is concerned with the functional form of the perturbed metal potential V_m'. Calculations of E_φ for various atomic configurations are given in Sec. III B. The level width Γ is calculated in Sec. III C. Finally, the tunneling matrix elements are calculated in Sec. III D.

A. Atom-Metal Interaction

In the literature of atom-metal interactions, it is known that one of the effects of the interaction is to push upwards the electronic energy levels of the atom, effectively decreasing their ionization potentials.[4–7,11,16,17] The physical reason for this is as follows. First consider the case of only an electron near the surface. The metal electrons readjust their positions to screen the field of the electron within the metal. A squashed exchange and correlation hole appears near the surface causing an effective attraction between the electron and the metal.[50,51] In the classical limit, this is the origin of the image force attraction $V_{e-\mathrm{im}} = -3.6/z$ eV with z the normal distance from the surface in angstroms and with the origin on the surface. However, if there is also an ion core present, the metal electrons will be attracted to the core in an effort to screen the field of the positive charged ion within the metal.[44] Within an image-force approximation the atomic electron sees a repulsive potential $V_{i-\mathrm{im}} \simeq 14.4/(2s+z)$ eV where s is the effective distance between the ion core and the image plane.[11] Details of this potential have been discussed elsewhere.[6] The system of image charges is shown in Fig. 6. Consequently, the total potential outside the metal seen by the atomic electron is

$$V_m' = 14.4\left(\frac{1}{2s-z} - \frac{1}{4(s-z)}\right) \text{eV}, \tag{20}$$

where we have now shifted the origin so that it is located on the ion core. The two terms in Eq. (20) can be combined to yield

$$V_m' = \frac{3.6}{s}\left(1-\frac{3}{2}\frac{z}{s}\right)\left(1-\frac{3}{2}\frac{z}{s}+\frac{1}{2}\frac{z^2}{s^2}\right)^{-1}. \tag{21}$$

If we expand the denominator of Eq. (21), take $z=r\cos\theta$, and keep all terms less than $O(r^3/s^3)$ we get

$$V_m' = \frac{3.6}{s}\left[1-\frac{1}{2}\frac{r^2}{s^2}\cos^2\theta+O\left(\frac{r^3}{s^3}\right)\right]$$

or in terms of spherical harmonics

$$V_m' = \frac{3.6}{s}\left[\left(1-\frac{1}{6}\frac{r^2}{s^2}\right)-\frac{1}{3}\frac{r^2}{s^2}\left(\frac{4\pi}{5}\right)^{1/2} Y_{2,0}(\theta,\varphi)+O\left(\frac{r^3}{s^3}\right)\right]$$

or (22)

$$V_m' \approx \frac{3.6}{s}\left[1-\frac{1}{3}\frac{r^2}{s^2}\left(\frac{4\pi}{5}\right)^{1/2} Y_{2,0}(\theta,\varphi)+\cdots\right],$$

when $\langle r_{\mathrm{av}}\rangle < s$ as it is in the cases considered here. It is felt that truncation of the sum at this point is valid for the following reasons. The operator V_m' will appear in matrix elements involving very localized atomic functions. These functions certainly will be localized to a region in which $\langle r\rangle < s$ since typically $s \approx 3$ Å.[11] Thus the higher-order terms would produce smaller matrix elements. Furthermore, as will be seen soon, angular momentum selection rules will eliminate most of the higher-order terms. Thus Eq. (22) gives the effective metal potential outside the surface that we will deal with in Secs. III B and III C.

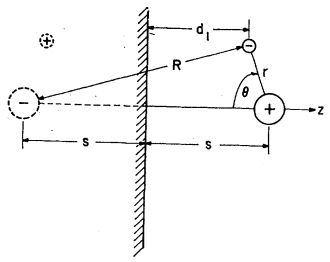

FIG. 6. Classical picture of the atom and the image charges it induces in the metal.

B. Determination of E_φ

The simplest case to consider first is for single-electron energy levels. We take the atomic wave function in the form $|a_0\rangle = C|u_{n,l}(r)\rangle|Y_{l,m}(\theta,\varphi)\rangle$. The value of $E_\varphi = \mathcal{E}_{nlm}+\Delta E$ is simply obtained through

$$\Delta E = \langle a_0|V_m'|a_0\rangle$$

$$= \frac{3.6}{s}\langle a_0|a_0\rangle - \frac{3.6}{s}\times\frac{1}{3}\left(\frac{4\pi}{5}\right)^{1/2}$$

$$\times C^2\langle u_{n,l}(r)\left|\frac{r^2}{s^2}\right|u_{n,l}(r)\rangle\langle Y_{l,m}|Y_{2,0}|Y_{l,m}\rangle. \tag{23}$$

Strictly speaking, the limits of integration should be restricted to only the outside of the metal. However, since most of the atomic wave function is well localized outside, only a small error will be introduced by letting the integrations range over all space. The resulting simplifications in calculations seem well worth this approximation. With this assumption, $\langle a_0|a_0\rangle = 1$ independent of the atomic state. Thus all energy levels are shifted an equal amount $\Delta\mathcal{E}_0 \equiv 3.6/s$. However, de-

[50] H. J. Juretschke, Phys. Rev. 92, 1140 (1953).
[51] J. W. Gadzuk, Surface Sci. 11, 465 (1968).

pending on the angular momentum state of the electron, the higher-order term could be important. Group-theoretical considerations give the general result that the integral of three spherical harmonics is related to the tabulated Gaunt coefficients which are certain products of Clebsch-Gordan coefficients.[52] The angular integral is thus given by

$$\langle Y_{l,m}|Y_{2,0}|Y_{l',m'}\rangle=\frac{1}{(2\pi)^{1/2}}\left(\frac{2l+1}{2}\right)^{1/2}c^l(20,l'm'), \quad (24)$$

where the Gaunt coefficient is nonvanishing only for $m=m'$ and $|l'-2|\leq l\leq l'+2$. For instance, if the ground state is an s state so that $l=l'=0$, then $c^0(20,00)=0$ and $\Delta E_s=\Delta\mathcal{E}_0$. On the other hand, for a d state $l=l'=2$, $c^2(20,20)=2/7$, and thus

$$\langle Y_{20}|Y_{20}|Y_{20}\rangle=(5/2\pi)^{1/2}/7.$$

Under these circumstances, the energy shift of the d state, from Eq. (23) is

$$\Delta E_d=\Delta E_0-\frac{3.6}{s}\frac{2}{21}\langle u_{n,2}(r)|r^2/s^2|u_{n,2}(r)\rangle. \quad (25)$$

As a result of the negative sign in the second term, the shift in the d state is not as great as an s state. Thus the splitting between an s state and a d state in an atom will appear smaller when the atom is sitting on a surface than when the atom is not perturbed. This is physically tenable when one considers that the d electron is more tightly bound to the ionic core. Thus it cannot feel as great a perturbation and hence its shift is not as large.

The quantity we are most interested in here is the change in the s-d splittings $\Delta E_{s\text{-}d}=\Delta E_d-\Delta E_s$. To get a rough idea of this change, the radial integral must be performed. We use as an order-of-magnitude estimate, Slater functions for the radial wave functions.[53] Thus $Cu_{n,2}(r)=Cr^{n-1}e^{-ar}$ with $a\approx(n-1)/r_{\rm av}$ where $r_{\rm av}$ is approximately some sort of shell radius.[54] The normalization constant is obtained by requiring

$$|C|^2\int|u_{n,2}(r)|^2r^2\,dr=1.$$

As an example consider a $5d$ level. Performing the integral in Eq. (25) yields

$$\Delta E_{s\text{-}d}=-\Delta E_0(3.14/s^2a^2), \quad (26)$$

when s is in Å and a in Å^{-1}. For reasonable values of $a\approx1.5$ Å^{-1}, $s\sim3$ Å, and $\Delta E_0\approx1$ eV the levels come closer together by a few tenths of an eV, a phenomenon we will see experimentally later. We will not totally rely, however, on the calculated values for $\Delta E_{s\text{-}d}$ treating this parameter more as an adjustable constant.

[52] M. Tinkham, *Group Theory and Quantum Mechanics* (McGraw-Hill Book Co., New York, 1964), p. 175.
[53] J. C. Slater, Phys. Rev. **36**, 57 (1930).
[54] K. S. Pitzer, *Quantum Chemistry* (Prentice-Hall, Inc., Englewood Cliffs, N. J., 1953), p. 82.

The next thing to consider is the effect of the surface perturbation on simple two-electron levels. Using the properly symmetrized product functions, we find the change in the total energy for an ns^2 ground state is simply

$$\Delta E_{ns^2}{}^{\rm tot}=2\langle u_{n,s}|V_m'|u_{n,s}\rangle$$

and thus the change per electron is the same as in the single-electron atom.

For the $6s5d$ singlet and triplet states, the change in total energy is

$$\Delta E_{6s5d}{}^{\rm tot}=\langle 6s|V_m'|6s\rangle+\langle 5d|V_m'|5d\rangle.$$

It is also worth noting that ΔE_{6s5d} is the same for both the singlet and triplet state so an experimental observation of these levels in resonance tunneling should see the same triplet-singlet splitting as in the isolated atom. This point will also be returned to when we discuss the data.

Lastly we note that in a resonance-tunneling experiment in which the initial and final state of the adsorbate is a $6s$ singly charged ion, as we believe to be the case for Ba, the tunneling electron going through one of the $6s5d$ states will be in the $5d$ configuration and thus will see a shift $\Delta E=\langle 5d|V_m'|5d\rangle$. Consequently, the splitting between the $6s^2$ and $6s5d$ states will be decreased as in the single-electron atom, this decrease being given by Eq. (26).

C. Determination of Γ

Quite detailed calculations for the lifetime broadening of single-electron s levels mixing with metal states at the surface have previously been given.[4–11] Little consideration, however, has been given to the lifetime effects on higher-angular-momentum states. From calculations[4–7] and experiment[24] it is now believed that an s state will acquire a width of about 1 eV. Due to the spatial contraction of a $(n-1)d$ state relative to an ns state, we should expect that $\Gamma_{(n-1)d}<\Gamma_{ns}$. In order to evaluate the current-enhancement factor in Eq. (19), an idea of the d level width relative to the s level is necessary. From Eq. (10) and past work it can be seen that Γ is proportional to the square of the matrix element of V_m' between the atom and metal state. The ratio of d to s level widths is thus

$$\frac{\Gamma_d}{\Gamma_s}=\frac{|\langle m|V_m'|5d\rangle|^2}{|\langle m|V_m'|6s\rangle|^2}\equiv R_\Gamma. \quad (27)$$

The major task in evaluating Eq. (27) is obtaining the matrix elements $M_5\equiv\langle m|V_m'|6s\rangle$ and $M_6\equiv\langle m|V_m'|5d\rangle$. We now address ourselves to this task.

For metal wave functions outside the metal we take simple damped exponentials,

$$|m\rangle=c_me^{-kz'}$$

with c_m a normalization constant which is not important

since we take ratios in Eq. (27). The propagation constant $k \approx [(2m/\hbar^2)(E_F+\varphi_e-E)]^{1/2}$, with E the electron kinetic energy inside the metal with the zero at the bottom of the conduction band. Transverse momentum is neglected here for the following reason. Since the tunneling depends upon the normal energy, for a given total energy those electrons with all their momentum directed normally will be much more important in tunneling processes than those with a significant amount of transverse momentum.[35] This is a simplifying approximation which can in principle be eliminated if it was deemed necessary. The coordinate origin has been put at the metal surface. If we transform to an origin at the atom center, then $z'=s+z$ and

$$|m\rangle = c_m e^{-ks} e^{-kz}. \tag{28}$$

This state can be expanded as a sum of spherical Bessel functions and spherical harmonics as follows. It is well known that

$$e^{ikz} = \sum_l [4\pi(2l+1)]^{1/2} i^l j_l(kr) Y_{l,0}(\theta,\varphi),$$

with j_l a spherical Bessel function of order l. Letting $k \rightarrow ik$ and realizing that $j_l(ikr) = e^{il\pi/2} j_l(kr)$,[55] we can then write Eq. (28) as

$$|m\rangle = c_m e^{-ks} \sum_l [4\pi(2l+1)]^{1/2} (-1)^l j_l(kr) Y_{l,0}(\theta,\varphi). \tag{29}$$

As before, the s state is

$$|6s\rangle = c_s u_{6,0}(r) Y_{00}(\theta,\varphi).$$

The potential V_m' is given in Eq. (22). Consequently, the matrix element M_5 can be written as

$$M_5 = c_m c_s e^{-ks} \frac{3.6}{s} \sum_l [4\pi(2l+1)]^{1/2} (-1)^l \times \left[\int r^2 j_l(kr) u_{6,0}(r)\, dr \int Y_{00} Y_{l,0}\, d\Omega - \frac{1}{3}\left(\frac{4\pi}{5}\right)^{1/2} \frac{1}{s^2} \times \int r^4 j_l(kr) u_{6,0}(r)\, dr \int Y_{l,0} Y_{2,0} Y_{00}\, d\Omega \right]. \tag{30}$$

The first spherical harmonic integral is simply $\delta_{l,0}$. The second one is $(4\pi)^{-1/2}\delta_{l,2}$. Thus Eq. (30) becomes

$$M_5 = c_m c_s e^{-ks} \frac{3.6}{s} (4\pi)^{1/2} \left(\int r^2 j_0(kr) u_{6,0}(r)\, dr - \frac{1}{3s^2} \int r^4 j_2(kr) u_{60}(r)\, dr \right) \equiv c_m c_s e^{-ks} \frac{3.6}{s} (4\pi)^{1/2} \left(I_1 - \frac{1}{3s^2} I_2 \right). \tag{31}$$

We will return to an evaluation of the integrals shortly.

[55] *Handbook of Mathematical Functions*, National Bureau of Standards Applied Mathematics Series 55 (U. S. Government Printing Office, Washington, D. C., 1965), p. 439.

The matrix element with the $5d$ state, M_6 is obtained in a similar manner. The $5d$ wave function is

$$|5d\rangle = c_d u_{5,2}(r) Y_{2,0}(\theta,\varphi).$$

Thus M_6 is

$$M_6 = c_m c_d e^{-ks} \frac{3.6}{s} \sum_l [4\pi(2l+1)]^{1/2} (-1)^l \times \left[\int r^2 j_l(kr) u_{5,2}(r)\, dr \int Y_{l,0} Y_{00} Y_{2,0}\, d\Omega - \frac{1}{3}\left(\frac{4\pi}{5}\right)^{1/2} \frac{1}{s^2} \int r^4 j_l(kr) u_{5,2}(r)\, dr \times \int Y_{l,0} Y_{2,0} Y_{20}\, d\Omega \right]. \tag{32}$$

Here the first spherical harmonic integral is $(4\pi)^{-1/2}\delta_{l,2}$. The second spherical harmonic integral is given in terms of the Gaunt coefficients of Eq. (24). The result is

$$\langle Y_{l,0} | Y_{2,0} | Y_{20} \rangle = \frac{1}{(2\pi)^{1/2}} \left(\frac{2l+1}{2}\right)^{1/2} c^l(20,20).$$

The only nonvanishing coefficients are $c^0(20,20)=1$, $c^2(20,20)=2/7$, and $c^4(20,20)=2/7$. Consequently, Eq. (32) reduces to

$$M_6 = c_m c_d e^{-ks} \frac{3.6}{s} (4\pi)^{1/2} \left[\left(\frac{5}{4\pi}\right)^{1/2} \int r^2 j_2(kr) u_{5,2}(r)\, dr - \frac{1}{3s^2\sqrt{5}} \int r^4 j_0(kr) u_{5,2}(r)\, dr - \frac{2\sqrt{5}}{21s^2} \int r^4 j_2(kr) u_{5,2}(r)\, dr - \frac{3}{7(\sqrt{5})s^2} \int r^4 j_4(kr) u_{5,2}(r)\, dr \right]$$

or

$$M_6 \equiv c_m c_d e^{-ks} \frac{3.6}{s} (4\pi)^{1/2} \left[\left(\frac{5}{4\pi}\right)^{1/2} I_3 - \frac{1}{3s^2\sqrt{5}} I_4 - \frac{2\sqrt{5}}{21s^2} I_5 - \frac{3}{7(\sqrt{5})s^2} I_6 \right]. \tag{33}$$

In a straightforward manner, the d to s level width from Eqs. (27), (32), and (33) is

$$R_\Gamma = \frac{c_d^2}{c_s^2} \left[\left(\frac{5}{4\pi}\right)^{1/2} I_3 - \frac{1}{3s^2\sqrt{5}} I_4 - \frac{2\sqrt{5}}{21s^2} I_5 - \frac{3}{7(\sqrt{5})s^2} I_6 \right]^2 \times \left(I_1 - \frac{1}{3s^2} I_2 \right)^{-2}. \tag{34}$$

As before, the radial functions are taken to be Slater functions so $u_{6,0}(r) = r^5 e^{-a_s r}$ and $u_{5,2}(r) = r^4 e^{-a_d r}$. All of

the radial integrals can be put into a standard form of a regular Bessel function of half-integer order times its argument raised to some power times an exponential. Then the integrals are Laplace transforms of this quantity which are exactly solvable in terms of Gaussian hypergeometric functions.[56] However, these functions depend upon four variables and have thus not been tabulated to any extent. We will invoke an approximation instead. For the energy ranges of interest in the present experiments $k\approx 1.2$ Å^{-1}. The average radius and hence the maximum in $r^{(n-1)}e^{-ar}$ occurs at $r\approx 2$ Å. Thus the integral d is significant only for $kr\sim 2$ which somewhat justifies using the asymptotic form for the spherical Bessel functions, $j_l(kr)\rightarrow (kr)^l/(2l+1)!!$ when $l\neq 0$. For $l=0$ we use the exact form $j_0(kr)=\sin(kr)/kr$. Using this approximation and performing the integrations, we get

$$I_1=\frac{\Gamma(7)}{k^8(\beta_s{}^2+1)^7}(7\beta_s{}^6-35\beta_s{}^4+21\beta_s{}^2-1), \tag{35a}$$

$$I_2\simeq\frac{\Gamma(12)}{15k^{10}\beta_s{}^{12}}, \tag{35b}$$

$$I_3=\frac{\Gamma(9)}{15k^7\beta_d{}^9}, \tag{35c}$$

$$I_4=\frac{\Gamma(8)}{k^9(\beta_d{}^2+1)^8}(8\beta_d{}^7-56\beta_d{}^5+56\beta_d{}^3-8\beta_d), \tag{35d}$$

$$I_5=\frac{\Gamma(11)}{15k^9\beta_d{}^{11}}, \tag{35e}$$

$$I_6=\frac{\Gamma(13)}{945k^9\beta_d{}^{13}}. \tag{35f}$$

Here the quantities $\beta_s=a_s/k$ and $\beta_d=a_d/\mathrm{k}$ have been introduced. With regards to the asymptotic approximation of the Bessel function, as mentioned I_1 and I_4 are exact as they stand. Use of the exact functions in the other integrals would somewhat reduce their values. As a result of the approximations, the actual broadening ratio would probably tend to be somewhat smaller than what we have calculated here and as such R_Γ obtained from Eqs. (34) and (35a)–(35f) will be an upper limit.

Finally, we have for the normalization constants $c_d=[(2a_d)^{11}/\Gamma(11)]^{1/2}$ and $c_s=[(2a_s)^{13}/\Gamma(13)]^{1/2}$.

The absolute value of the s-level broadening will be taken from the more detailed calculations in Ref. 6. These turn out to be roughly $\Gamma_s\approx 1$ eV. The widths for d levels will be obtained through $\Gamma_d=R_\Gamma\Gamma_s$ with R_Γ given by Eqs. (34) and (35) and Γ_s taken from Ref. 6. Numerical evaluation of these results will appear in Sec. IV.

[56] G. E. Roberts and H. Kaufman, *Tables of Laplace Transforms* (W. B. Saunders Co., Philadelphia, 1966), p. 60.

D. Determination of Tunneling Matrix Elements

The final item to be treated in this section is the evaluation of the tunneling matrix elements of Eqs. (18a)–(18e) or at least some suitable approximation to them. Consistent with our strategy of using the Oppenheimer perturbation scheme only to calculate relative matrix elements of d to s electron transitions, we will evaluate the absolute transition probabilities involving free, metal, and s electrons within Harrison's WKB approximation.[35] From Eq. (8), of his paper, the tunneling matrix element for an electron going through a barrier region in which $z_a\leq z\leq z_b$, is

$$M_{a-b}=\frac{\hbar^2}{2m}\left(\frac{k_z}{L_a}\right)^{1/2}_{z=a}\left(\frac{k_z}{L_b}\right)^{1/2}_{z=b}\exp\left(-\int_{z_a}^{z_b}|k_z|\,dz\right). \tag{36}$$

We have assumed a free-electron band structure in the metal. L_a and L_b are the lengths associated with the allowed regions to the left and right of the barrier and $k_{z=a}$ and $k_{z=b}$ are the propagation constants

$$k_z=\{(2m/\hbar^2)[E_\mathrm{F}+\varphi_e-E-eF(z+s)]\}^{1/2}$$

evaluated at the appropriate values of z. In the assumed triangular barrier in field emission we will assume that the integrand in the exponent can be replaced by an average k value such that

$$\int_{z_a}^{z_b}|k_z|\,dz=\bar{k}(z_b-z_a)$$

with

$$\bar{k}=\tfrac{1}{2}[(2m/\hbar^2)(E_F+\varphi_e-E)]^{1/2}.$$

The tunneling process in the presence of the atomic potential well, as shown in Fig. 3, is taken to be describable as two WKB tunneling probabilities through the reduced double barrier when an s state is the intermediate atomic state. Then using Eq. (36) for the tunneling matrix elements, Eqs. (18a)–(18c) take the form

$$M_0=\frac{\hbar^2}{2m}\left(\frac{\bar{k}_z}{L_\mathrm{met}}\right)^{1/2}_{z=-s}\left(\frac{\bar{k}_z}{L_\mathrm{free}}\right)^{1/2}_{z=sT-s}e^{-\bar{k}sT}, \tag{37a}$$

$$M_1=\frac{\hbar^2}{2m}\left(\frac{\bar{k}_z}{L_\mathrm{atom}}\right)^{1/2}_{z=+w}\left(\frac{\bar{k}_z}{L_\mathrm{free}}\right)^{1/2}_{z=sT-s}e^{-\bar{k}(sT-s-w)}, \tag{37b}$$

$$M_2=\frac{\hbar^2}{2m}\left(\frac{\bar{k}_z}{L_\mathrm{atom}}\right)^{1/2}_{z=-w}\left(\frac{\bar{k}_z}{L_\mathrm{met}}\right)^{1/2}_{z=-s}e^{-\bar{k}(s-w)}. \tag{37c}$$

In the expression for the enhancement factor, Eq. (19), these terms appear in the combination

$$T_s=\frac{M_1M_2}{M_0}=\frac{\hbar^2}{2m}\frac{(\bar{k}_z)_{z=-w}{}^{1/2}(\bar{k}_z)_{z=+w}{}^{1/2}}{L_\mathrm{atom}}e^{2\bar{k}w}.$$

Since $(k_z)_{z=-w}\approx(k_z)_{z=+w}\approx(k_z)_{z=0}$ and with $L_{\text{atom}}=2w$, the simple result

$$T_s=\tfrac{1}{4}(\hbar^2/2m)(k/w)e^{kw} \tag{38}$$

obtains, where now $k=[(2m/\hbar^2)(E_F+\varphi_e-E)]^{1/2}$. For reasonable values of k and w, this quantity indeed is a slowly varying function of energy of order unity times an exponential, as stated earlier in this paper and in the preliminary account of this work.[24]

The tunneling matrix elements involving d states, Eqs. (18d)–(18e) are obtained through the Oppenheimer technique. The d element is given by the ratio of the d to s matrix elements in the Oppenheimer approximation times the s probability within the WKB approximation. Thus

$$M_3=\left(\frac{\langle f|V_F|5d\rangle}{\langle f|V_F|6s\rangle}\right)_{\text{Opp}}\langle f|V_f|6s\rangle_{\text{WKB}}\equiv R_{d-s}{}^fM_1$$

and

$$M_4=\left(\frac{\langle 5d|V_F|m\rangle}{\langle 6s|V_F|m\rangle}\right)_{\text{Opp}}\langle 6s|V_F|m\rangle_{\text{WKB}}\equiv R_{d-s}{}^mM_2,$$

where now M_1 and M_2 are given by Eqs. (37b)–(37c). As with the s probabilities, these terms always appear in the combination

$$T_d=M_3M_4/M_0=R_{d-s}{}^fR_{d-s}{}^mT_s\equiv R_{\text{tot}}T_s. \tag{39}$$

To proceed, the rather grim task of calculating the R factors must be faced. If we go through a similar expansion procedure as that from Eqs. (28)–(34) in which the potential

$$V_F=eFs(1+z/s)=eFs[1+(\tfrac{4}{3}\pi)^{1/2}(r/s)Y_{1,0}(\theta,\varphi)],$$

the result for R_{tot} identified in Eq. (39) is

$$T_{\text{tot}}=\frac{c_d}{c_s}\frac{[-(2/s\sqrt{15})I_7+(\sqrt{5})I_8-(3/s\sqrt{5})I_9]^2}{[I_{10}-(1/s)I_{11}]^2}, \tag{40}$$

where the following integrals are to be determined:

$$I_7=\int f_{5,2}(r)j_1(kr)r^3\,dr,$$

$$I_8=\int f_{5,2}(r)j_2(kr)r^2\,dr,$$

$$I_9=\int f_{5,2}(r)j_3(kr)r^3\,dr,$$

$$I_{10}=\int f_{6,0}(r)j_0(kr)r^2\,dr,$$

$$I_{11}=\int f_{6,0}(r)j_1(kr)r^3\,dr.$$

The integrals, when evaluated within the same approximations as those leading to Eqs. (36a)–(36d), are

$$I_7=\Gamma(9)/3k^8\beta_d{}^9, \tag{41a}$$

$$I_8=\Gamma(9)/15k^7\beta_d{}^9, \tag{41b}$$

$$I_9=\Gamma(11)/105k^8\beta_d{}^{11}, \tag{41c}$$

$$I_{10}=[\Gamma(7)/k^8(\beta_s{}^2+1)^7](7\beta_s{}^6-35\beta_s{}^4+21\beta_s{}^2-1), \tag{41d}$$

$$I_{11}=\Gamma(10)/3k^9\beta_s{}^{10}. \tag{41e}$$

With the results of Eqs. (38)–(40) and (41a)–(41e) we are now in a position to perform numerical calculations of the s and d resonance transmission functions and the subsequent current-enhancement factor, Eqs. (13) and (19). The numerical aspects of the problem together with a comparison with experimental data and general discussion appears in Secs. IV and V.

IV. NUMERICAL RESULTS

A. Zr

The simplest case to consider first is the single-level Zr resonance. Preliminary results of the Zr on tungsten case have appeared.[24] Zr has a $5s^2$ level at 6.84 eV below the vacuum level when the atom is isolated. In accord with Eq. (23), in the adsorbed state we would expect this level to shift upwards by an amount $\Delta E\approx 3.6/s$ eV ≈ 1.6 eV for a reasonable value of atom-metal separation $s\approx 2.5$ Å. Furthermore, the detailed calculations of s-level broadening due to the atom-metal configuration interaction[4–7,11] suggest that a broadening $\Gamma\sim 1$ eV would be reasonable. The width of the atomic potential well w should be a bit less than some sort of atomic radius ≈ 1.5 Å. Thus to calculate the single s-level enhancement given by Eqs. (13) and (38), all the necessary parameters can be specified in an *ab initio* sense. However, we shall be a bit more empirical and just use various combinations of w and Γ to see what R values result. The curve for $w=1$ Å and $\Gamma=1$ eV is shown in Fig. 7 together with the experimental points measured by Plummer *et al.*[24,26] Because of the width and the position of the Zr resonance, it was not possible to see this structure in a single TED as depicted in Fig. 2(b), but instead a roundabout technique of adsorbing the Zr on different surface planes and then comparing the slopes of the Fowler-Nordheim plots with the slopes of the TED was required, as outlined selewhere.[24,57] Possible complications due to different charge states and different broadening and shift parameters on the different crystal planes have thus been neglected in the analysis of the Zr resonance.[11] However, the curve does seem to contain the experimental points within the experimental uncertainties. It is noteworthy that the values of Γ changed rather slowly as w was varied over a significant range.

[57] E. W. Plummer, H. E. Clark, and R. D. Young, Fifteenth Field Emission Symposium, Bonn, Germany, 1968 (unpublished).

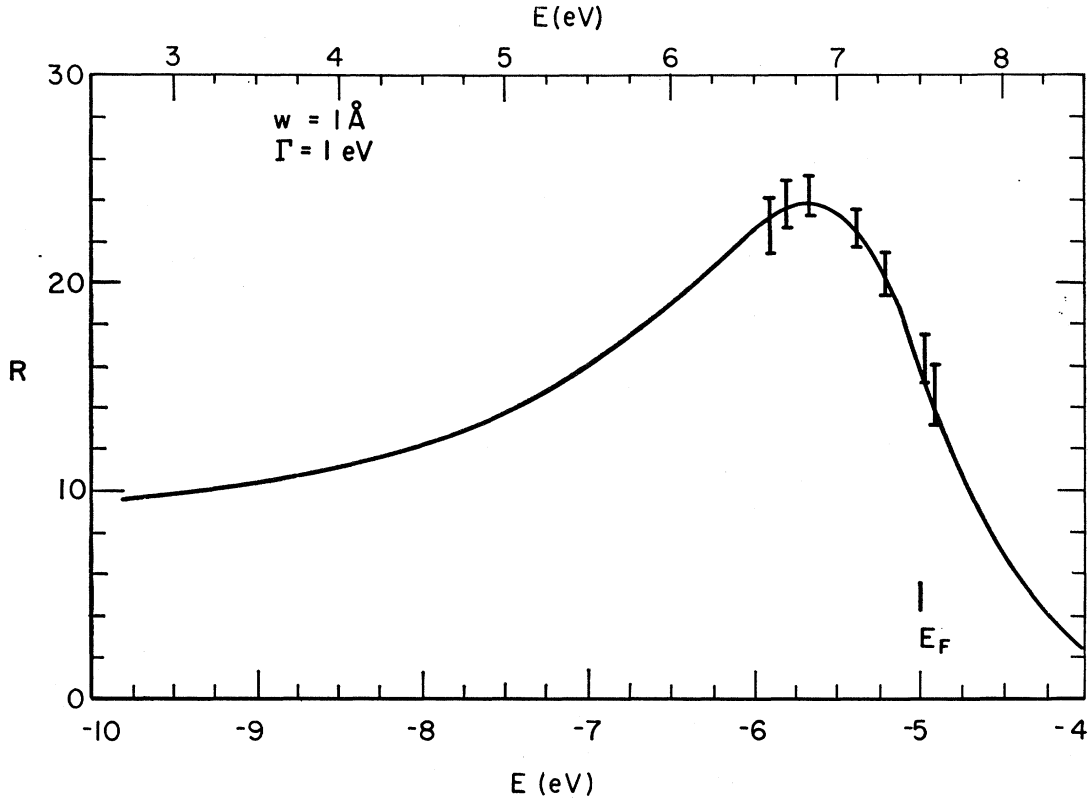

FIG. 7. Theoretical and experimental values of the enhancement factor as a function of energy for Zr on tungsten. The energy scale of the bottom is taken with a zero at the vacuum potential whereas the scale at the top is taken with a zero at the bottom of the conduction band.

The absolute value of the enhancement factor seemed to have a maximum falling somewhere between $20 \leq R_{\max} \leq 100$. By requiring the theoretical value of R to assume this value at $E = E_\varphi$ and by specifying a choice of the potential well width w, the value of Γ is uniquely determined through $\Gamma = [T_s(E_\varphi; w)]/[R_{\max}(E_\varphi) - 1]^{1/2}$. Consequently, we are really doing only a two-parameter fit. We believe though that, owing to the relative insensitivity of the final result for Γ on our choice of w, the assignment of the value of Γ is credible. It seems fair to conclude that the experimental current-enhancement factors for resonance tunneling through Zr on tungsten, when analyzed within the context of the present theory yield values for the atomic level $\Gamma \approx 1$ eV in good agreement with predicted values of the order of 1 eV.[5,6]

It should also be mentioned that the peak in R does not occur at the atomic-band center but is shifted down from the vacuum potential by about 0.4 eV. This results from the rather broad value of Γ in the Lorentzian. The Lorentzian does not completely dominate the energy dependence of R and the energy-dependent tunneling probabilities play a more important role than might be expected.

The shapes of the R-versus-E curves are in rough agreement with the shapes calculated by DA.[1] However, it must be remembered that in the DA theory, transmission functions were evaluated by matching wave functions at boundaries, a procedure which has strong quantum-mechanical reflection effects built into it. His reflection and transmission calculations were done on model potentials with sharp barriers, a system whose transmission effects are radically different from systems with slightly rounded potential barriers. Thus we should not expect quantitative agreement between experiment or the present theory when compared with the calculations of DA.

We should note also that the enhancement factor does not go nicely to zero as the energy goes deeper into the band. This also results from the fact that the decreasing value of the Lorentzian does not dominate the enhancement factor. In fact the energy-dependent tunneling factor which increases exponentially as the square root of energy as the energy goes down into the band could cause the R factor to begin rising quite strongly below the maximum value of R. Although the Zr data are not sufficiently complete to confirm this prediction, Plummer and Young did note this effect in some of the Ba and Ca results. The experimental enhancement factors displayed local maxima corresponding to the atomic spectra, but as one went to the low-energy tails of the TED, below the atomic energy levels, the R values in

some circumstances did seem to diverge exponentially. This behavior is unexpected from the reported numerical results of DA[1] but could be understood within the context of the present theory.

B. Ba

The real *tour de force* in the present theory is the application of these results to the interpretation of Plummer and Young's Ba on tungsten data in which three resonances are observed.[26] Atomic spectroscopy tables show that the Ba atom has a $6s^2$ ground state at 5.2 eV, a triplet ^3D $6s5d$ excited state between 4.03 and 4.10 eV and a singlet ^1D $6s5d$ state at 3.8 eV. It was hoped that under the perturbation of the surface on this atom, some manifestation of these states as structure in the TED from resonance-tunneling effects could be observed and subsequently interpreted. As will be seen, our expectations were satisfied.

We mentioned earlier that the spatial contraction of a $5d$ state relative to a $6s$ state might reduce the broadening of the $6s5d$ levels relative to the broadening of the $6s^2$ level in analogy with the reduced widths of tight-binding d bands compared to s bands in noble and transition metals.[58] For example, in Cu, bands resulting from $3d$ states are roughly one-tenth the width of $4s$ bands. We might expect a similar situation to result in the case of $5d$ Ba levels compared to $6s$ levels. In Sec. III, Eqs. (35) and (36a)–(36f) were derived. Equation (34) is the expression R_Γ for the ratio of $6s5d$ to $6s^2$ level widths when the Ba atom is adsorbed on a metal surface. These equations have been numerically evaluated for reasonable choices of system parameters. We have taken $\varphi_e=4.4$ eV, $E_F=7.5$ eV, $s=3$ Å, and have used various values for a_s and a_d, the parameters in the Slater function. These values of a can be crudely related to atomic radius parameters and should be of the same order as an inverse radius times the principal quantum number minus one.[54] The numerical results of R_Γ as a function of the position of the energy level are shown in Fig. 8 for some choices of a_s and a_d. In all cases in which the $5d$ orbit is roughly the same size as the $6s$ orbit, the ratio of level widths is of order 0.1–0.2, a result which is both satisfying and expected. Physically this results from the fact that when the electron tunnels from the atom to the metal, the effective barrier for the d electron is thicker than for the s electron. The d electron must tunnel not only through the Coulomb and surface barriers but also through a centrifugal barrier of the form $+l(l+1)/r^2$. Consequently, its tunneling probability and hence natural linewidth is significantly reduced compared to lower-angular-momentum states. Mathematically the result obtains from the fact that the tunneling matrix elements involving d states pick out only higher partial waves in the expansion of the final state which have a smaller amplitude in the region of the atomic core where the overlap must occur. This can be seen in the asymptotic expansion of the spherical Bessel function $j_l(kr) \rightarrow (kr)^l/(2l+1)!!$ for kr reasonably small. This result is in accord with the

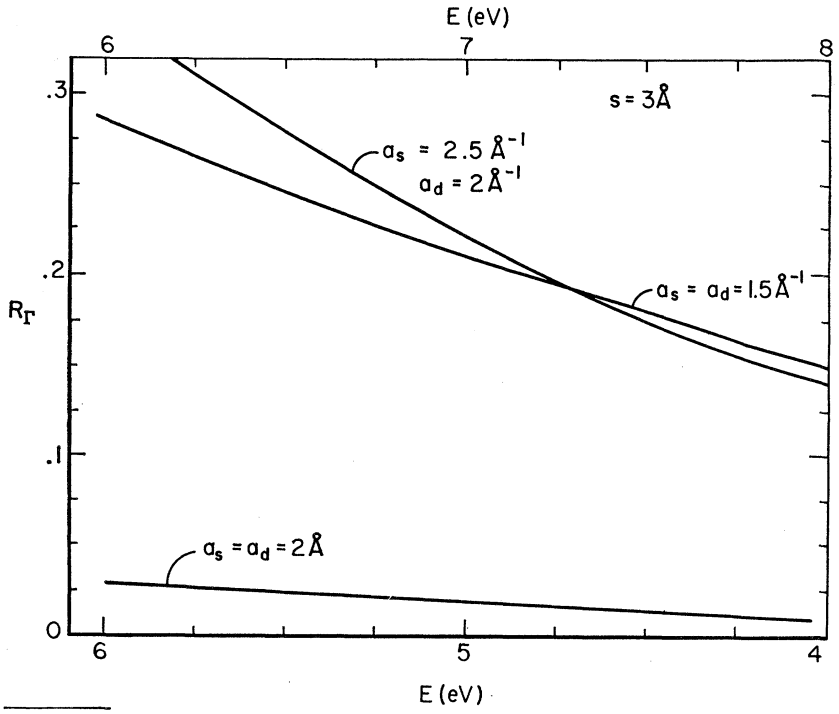

FIG. 8. Ratio of d to s level widths as a function of energy. The scale is the same as in Fig. 7.

[58] L. Hodges, H. Ehrenreich, and N. D. Lang, Phys. Rev. 152, 505 (1966).

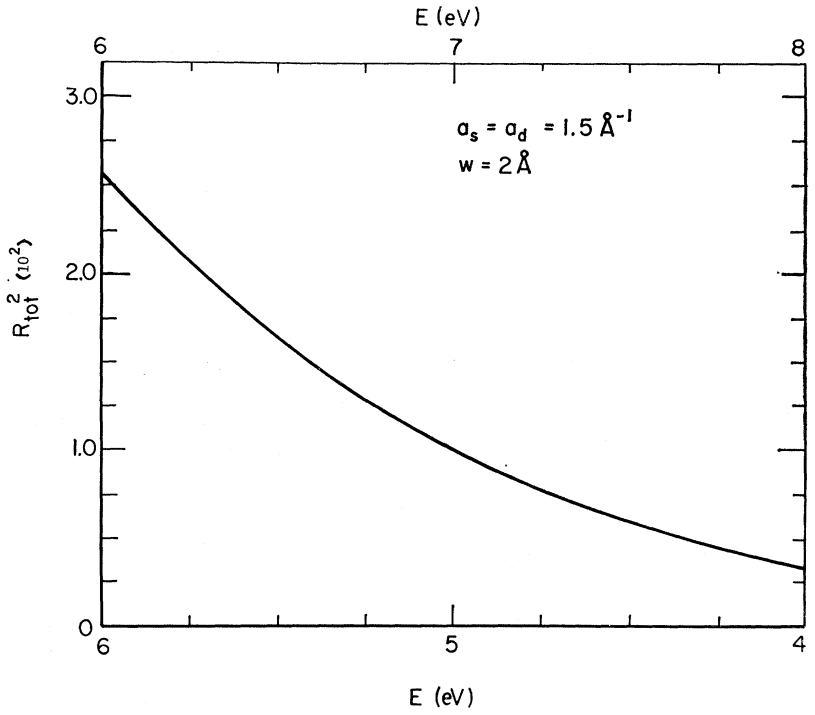

FIG. 9. Ratio of resonance-tunneling probabilities involving d or s intermediate states. The same scale as in Fig. 7 is used.

expected results from energy-band theory. As a final comment on the broadening, we note that both theoretical calculations[5,6] and the experimental data on Zr indicate s-level widths of the order of 1 eV. Consequently, d-level widths would be roughly 0.1 eV.

The determination of the enhancement factor involves two distinctly different modifications when treating resonant d states. First, knowledge of the d-level position and width is required. The width has just been discussed. Secondly, we must know the relative tunneling probability ratios of d to s resonant states. This has been expressed in Eqs. (40) and (41a)–(41e). The quantity $|R_{\rm tot}|^2$ gives the relative tunneling probabilities, which when used in conjunction with Eqs. (38) and (39) give the absolute d-level tunneling probabilities. In Fig. 9, $|T_{\rm tot}|^2$ is drawn as a function of energy for the same choice of parameters as in Fig. 8. Here we have taken $a_s = a_d = 1.5$ Å^{-1}, a choice which is both reasonable physically and also in accord with the values used in the calculation of R_Γ. These results show that the relative tunneling probability involving an intermediate d state is reduced by a factor of about 10^{-2} compared with the s tunneling channel. This again is reasonable for the same physical and mathematical reasons as was the reduced bandwidth. Also the total tunneling from metal to atom and then from atom to vacuum is a two-step process and thus involves a product of two reduction factors. Since the atom-to-metal factor which is similar to that in the Γ calculation is about 10^{-1}, the product of this times an atom-to-vacuum factor which also should be of order 10^{-1}, is of order 10^{-2} as calculated here. This is in good agreement with the ratio of d to s electron tunneling factors for electrons in noble and transition metals calculated elsewhere.[31] It is also interesting to note that Hagstrum has observed d-band tunneling in ion-neutralization experiments to be as much as $\sim 2\times 10^{-2}$ less probable than for s-band tunneling of electrons at the same energy.[59,60] Again the reasons for this are similar to our ideas, the d electrons are more localized and thus do not overlap electron states outside the metal as much, resulting in reduced tunneling probabilities.

As a preliminary comment before obtaining the enhancement factors we note that the narrow-band d levels would give a much greater peak height than the s levels if it were not for the fact that the Lorentzian for the d levels is moderated by the $R_{\rm tot}$ factor.

Finally we can combine Eqs. (19), (38)–(40), and 4(1a)–(41e) to obtain the expression for the Ba enhancement factor. The parameters used are $a_s = a_d = 1.5$ Å^{-1}, $s = 3$ Å, $w = 1.5$ Å, $E_F = 7.5$ eV, $\varphi_e = 4.4$ eV, $\Gamma_s = 0.75$ eV, and $\Gamma_d = 0.1$ eV. A number of points are worthy of note here. First, since both Ba and Zr have an ns^2 ground-state configuration, we might expect the atomic parameters and effective well widths to be larger for Ba, the larger atom. Coincidentally, in doing the numerical calculations, the only way that the theoretical Ba curves could be made to fit the data was by choosing a value

[59] H. D. Hagstrum and G. E. Becker, Phys. Rev. **159**, 572 (1967).

[60] W. E. Spicer, in *Optical Properties and Electronic Structure of Metals and Alloys*, edited by F. Abeles (North-Holland Publishing Co., Amsterdam, 1966), p. 312.

of w greater than the 1 Å needed for the Zr data, in accord with physical expectations. Secondly, Ba is a bigger atom than Zr and thus is farther from the surface. Thus we would expect it to be less perturbed by the metal, one manifestation of this being a smaller natural width of the virtual levels. Again there was no reasonable way in which we could make the theoretical curve agree with experiment unless we choose $\Gamma_{6s}{}^{\mathrm{Ba}}<\Gamma_{6s}{}^{\mathrm{Zr}}=1.0$ eV in agreement with physical expectations.

A problem resulted in choosing the values for E_φ, the positions of the atomic levels. The theoretical estimates given by Eqs. (23) and (26) predict that $\Delta E_{6s}\approx 0.95$–$1.0$ eV is reasonable. This is a smaller shift than for the Zr, in accord with the idea that Ba is a larger atom and thus less perturbed by the metal. We have taken $s_{\mathrm{Zr}}\approx 2.5$ Å whereas $s_{\mathrm{Ba}}\approx 3$ Å. However, Eq. (26) says that s-d splitting should decrease only of order 0.1 eV, whereas we find the decrease $\Delta E_{s-d}\approx 1$ eV. It is possible that for the $m=0$ d states, the d electron more effectively screens the ion core from the metal electrons and thus the repulsive part in the model potential, Eq. (20), is not as large. This would result in a much smaller d shift than s shift and consequently a greater value for ΔE_{s-d}. This remains a problem for the future. This anomaly forced us to be guided by the experimental results and thus we choose $\Delta E_{5d}=0$ in accord with the data. The theory does predict that the splitting between ^3D and ^1D will remain the same whether the atom is isolated or is on the surface, a fact seen experimentally. We are thus forced to use one arbitrary parameter $E_\varphi{}^{^3D}$ in our calculation but imagine that this problem can be cleared up by a more detailed calculation of the atom-metal interaction.

Another point should be brought up concerning the concept of the contracted $5d$ orbit. Cooper has provided the writer with numerical calculations of the Ba $5d$ atomic functions which indeed support the contentions of this paper. The accurate Hartree-Fock calculations show that the maximum in the radial $5d$ function occurs at a radius of about 1.4 Å, whereas the maximum of the $6s$ function occurs at 2.14 Å even though the $6s5d$ configuration is higher in energy than the $6s^2$ configuration.

Finally, the calculated and typical experimental enhancement factors for different crystal faces appear in Fig. 10.[26] The agreement between experiment and theory is compelling. The position of one of the d peaks has to

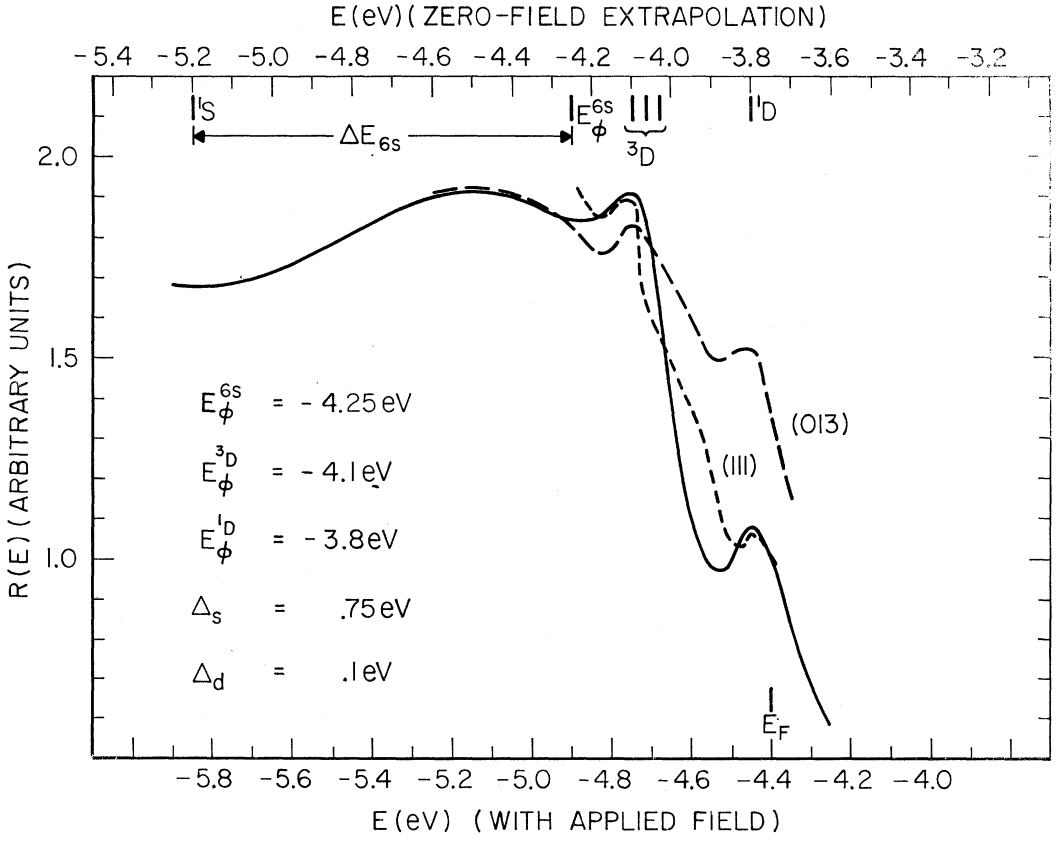

FIG. 10. Theoretical and experimental values of the enhancement factor and thus virtual-energy-level spectrum for Ba on tungsten. The magnitude of R is left arbitrary owing to experimental uncertainties but would generally fall in the range $10\lesssim R_{\max}\lesssim 10^3$. The scale on the bottom is that used in the experiment. The scale on the top is that resulting from an extrapolation to the zero-field limit. Note the positions of the unperturbed atomic levels and the position of E_φ.

some extent been determined by the arbitrary choice of $E_\varphi{}^{3D}$, but that is all that can be regarded as curve fitting. The absolute widths have been calculated from first principles. The relative heights of the peaks have also come out of the first-principles calculations, a fact which is felt to be a rather significant point in justifying the validity of the present approach to the resonance-tunneling phenomenon. In any event, the agreement between experiment and theory seems quite adequate to allow us to conjecture that in fact we do have a tool for doing atomic spectroscopy of atoms adsorbed on metal surfaces.

In Fig. 10, two different energy scales have been used. On the bottom, the energy scale of the experiment is used. This is the scale in which all atomic energies have been shifted down an amount eFs owing to the applied field. Plummer and Young estimate that the extrapolation to the zero-field situation will shift the scale upwards about 0.75 eV. The zero-field results are the ones to compare with the atomic spectrum. This scale and the atomic energy levels appear on the upper ordinate. The triplet states are too close together to resolve with the present energy analyzer.[61]

In performing the calculations, the relative peak heights were extremely sensitive to the choice of Γ_s and Γ_d. Thus with a change in Γ_d of 10%, the relative s to d heights changed significantly. However, the same situation was noted experimentally. The position of the peaks was extremely reproducible but their relative height varied greatly as can be seen by comparing the two experimental curves in Fig. 10. This could result from local microscopic differences in adsorption sites which would give rise to different level widths and thus the same sensitivity to these changes experimentally as theoretically. Also, in some cases, both experimentally and theoretically, the exponential divergence of the enhancement factor for energies below the d levels was observed as discussed briefly in Sec. IV A.

Although it might appear that there is a good deal of arbitrariness in the choices of the physical constants in the theory, we feel this is not the case. It cannot be proved that we have arrived at a unique solution to the problem, but after exhaustive numerical studies with various choices of constants, it is felt that the results forced us to zero in on the present set which are all physically reasonable.

In conclusion, for the specific case of Ba on tungsten we can say that in the zero-field limit a virtual $6s^2$ ground state at $E_\varphi{}^{6s}=4.25$ with $\Delta E^{6s}=0.95$ eV and $\Gamma_{6s}=0.75$ eV, a virtual ^3D $6s5d$ excited state at $E_\varphi{}^{3D}=4.10$ with $\Delta E^{3D}\approx 0$ and $\Gamma_{^3D}=0.1$ eV, and a virtual ^1D $6s5d$ excited state at $E_\varphi{}^{1D}=3.80$ with $\Delta E^{1D}\approx 0$ and $\Gamma_{^1D}=0.1$ eV have been seen in a resonance-tunneling experiment,[26] the results of which are mostly predictable in terms of the theory presented here. The theory is sufficiently simple and transparent that it should be accessible to future workers in the field, and the less than 0.5 sec of computer time or one-half hour of slide-rule time needed to generate structured curves such as in Fig. 10 makes it an economically as well as aesthetically pleasing exercise.

[61] R. D. Young and C. E. Kuyatt, Rev. Sci. Instr. **39**, 1477 (1968).

C. Ca

Although specific calculations have not been carried out for Ca on tungsten, some qualitative discussion should be put forth with regards to the compatibility of Plummer and Young's experimeneal results and the present theory. In the free-atom state, calcium has a $4s^2$ ground state at 6.1 eV and a $4s4p$ excited state at 4.25 eV. If the energy-level shifts of Ca, upon adsorption, are similar to those of Ba then the ground state should lie too low in energy to be meaningfully observed with the present integral energy analyzers used in experiments. However, the $4s4p$ state should shift upwards relative to the $6s5d$ Ba states and should be observable.

Indeed, the experimental results show what is expected. The $4s4p$ level is shifted upwards more than the Ba $6s5d$'s owing to the increased delocalization of the p states. From the theoretical calculations of linewidths we would expect the p level to be less broad than s levels but broader than d levels due to the angular momentum selection rules and the resulting nonvanishing matrix elements between the p state and only higher-order partial waves. This in fact is observed. The width of the $4s4p$ level appears to be roughly 0.3–0.5 eV falling in between the previously observed 1 eV s level and 0.1 eV d levels. The reader should go to Plummer and Young's paper for the display of these results.[26] Although not treated quantitatively, the experimental results of Ca on tungsten indicate that a $4s4p$ level exists at $E_\varphi\approx 3.85$ eV and $\Gamma_{4p}\approx 0.3$ eV, in accord with the expectations of the theory.

V. CONCLUSIONS AND DISCUSSION

The theory of resonance tunneling first elucidated by DA has been revisited.[1] In the new formulation of the problem, presented here, direct contact with previous concepts of virtual-surface-impurity states of atoms adsorbed on metal surfaces has been made. It has been shown how field-induced resonance tunneling through adsorbed atoms can be turned into a spectroscopy of the virtual atomic energy levels associated with the combined atom-metal system. The experimentally determined resonance curves obtained by Plummer and Young and presented in the preceding paper have been analyzed in terms of the theory presented here. We have quantitatively treated the cases of resonance tunneling involving both s- and d-like atomic virtual levels. For the most part, the calculations could be considered to be first-principles calculations. The agreement be-

tween theory and experiment appears very satisfactory. On the basis of the theory and experiment we have been able to make assignments of position and width of the atomic levels in Zr, Ba, and Ca adsorbed on tungsten surfaces which are experimentally accessible in the present field-emission experiments.

As pointed out by DA, the tremendous current enhancements resulting from resonance tunneling through adsorbed atoms can explain many anomalies in past field-emission studies.[62] In addition to the spectroscopic tool which we have used resonance tunneling for, the analysis of field-emission data in which atoms have been adsorbed on the surface will have to contain some aspects of resonance-tunneling effects in order to depict correctly what is physically occurring. It is felt that the particularly simple functional forms of the enhancement factor obtained in this paper will enable such a procedure to be carried out in a relatively easy manner.

It is also interesting to speculate on the possible role of resonance-tunneling spectroscopy in the theory of magnetic impurities. Newns has attempted to modify the Anderson theory of magnetic impurities such that it is applicable to surface impurities.[9,10,14] A spin-polarization analysis of field-emitted electrons[63] through a virtual-magnetic-impurity state on the surface might be possible in a resonance-tunneling experiment and could shed significant light on the validity of the theoretical ideas. This remains an interesting problem of the future.

As mentioned in Sec. I of this paper, present thinking on the microscopic level with regards to atom-metal interactions requires knowledge of the position E_φ and width Γ of the atomic energy levels in order that effective adsorbate charge, dipole moments, work-function changes, and binding energies can be calculated theoretically.[4–12] Resonance-tunneling spectroscopy provides just the tool needed for cataloging the virtual atomic levels. Not until significant headway is made in this rather involved task can we hope to come to a satisfactory quantitative understanding of the microscopic electronic properties of adsorption phenomena and thus be able to reliably predict macroscopic effects from microscopic considerations.

ACKNOWLEDGMENTS

Comments and stimulation from Dr. R. D. Young and J. W. Cooper and Professor U. Fano have been appreciated. Without the close collaboration of Dr. E. W. Plummer this study would have been impossible.

APPENDIX

In considering the zero-field impurity theory in Sec. II, it was suggested that writing the virtual-impurity-state wave function as a simple first-order perturbation-theory admixture with the metal states was equivalent to the Anderson impurity theory within a single-electron approximation. The major result of the approximation represented by Eq. (6) and outlined in greater detail in Refs. 5, 6, and 11 is that the original impurity level $\mathcal{E}_a^0$ becomes broadened and shifted such that the final virtual state has an energy $\mathcal{E}_a' = E_\varphi + i\Gamma$ with $\Gamma = 2\pi \sum_m \delta(E-E_m) |\langle m| V_m' |a_0\rangle|^2$. The electron occupation of the impurity state depends upon the position of this band relative to the occupied portion of the metal conduction band. In fact we can identify an impurity-state Green's function

$$G_{aa}^{\sigma}(\mathcal{E}) = 1/(\mathcal{E} - E_\varphi - i\Gamma) \tag{A1}$$

from which the impurity density of states

$$\rho_{aa}^{\sigma}(\mathcal{E}) = \frac{1}{2\pi} \mathrm{Im} G_{aa}^{\sigma}(\mathcal{E}) = \frac{1}{2\pi} \frac{\Gamma}{(\mathcal{E}-E_\varphi)^2 + \Gamma^2} \tag{A2}$$

is obtainable. The extra factor of 2 in the denominator enters as a result of what we call the single-electron approximation in which

$$\int_{-\infty}^{+\infty} \rho_{aa}(\mathcal{E})\, d\mathcal{E} = 1, \tag{A3}$$

where $\rho_{aa} = \sum_\sigma \rho_{aa}^{\sigma}$. If one was doing a full unrestricted Hartree-Fock treatment in which magnetic states were being sought, then the problem would be much more complicated. The effective occupation of the impurity level is

$$\begin{aligned} \langle n_a \rangle &= \int_{-\infty}^{E_F} \rho_{aa}(\mathcal{E})\, d\mathcal{E} \\ &= (1/\pi)[\tfrac{1}{2}\pi + \tan^{-1}(E_\varphi - \varphi)/\Gamma]. \end{aligned} \tag{A4}$$

In the final answer above, the zero of energy has been shifted to the vacuum potential outside the metal so that the upper limit at the Fermi level then becomes φ, the metal work function below the zero. For instance, in alkali atom adsorption $E_\varphi - \varphi$ is a negative number of the same order as Γ such that $\tan^{-1}(E_\varphi - \varphi)/\Gamma \approx -\frac{1}{4}\pi$. Thus $\langle n_a \rangle \lesssim 0.25$ and many of the ideas in the low-density approximation of Schrieffer and Mattis are relevant.[64] Although the alkaline earths have two-electron neutral states, many of the low-density single-electron-approximation ideas can be carried over.

The Anderson Hamiltonian is written as

$$\begin{aligned} H = \sum_\sigma \mathcal{E}_\varphi{}^{\sigma} n_{a\sigma} + \sum_{m,\sigma} \mathcal{E}_m n_{m\sigma} + \sum_{m,\sigma} (V_{am} c_{a\sigma}{}^{\dagger} c_{m\sigma} + \mathrm{H.c.}) \\ + U n_{a\sigma} n_{a-\sigma}, \end{aligned} \tag{A5}$$

where σ denotes spin, n_a and n_m are impurity and metal state occupation numbers, $c_a(c_a{}^{\dagger})$ and $c_m(c_m{}^{\dagger})$ are atom

[62] H. E. Clark and R. D. Young, Surface Sci. **12**, 385 (1968).
[63] G. Obermair, Z. Physik **217**, 91 (1968).
[64] J. R. Schrieffer and D. C. Mattis, Phys. Rev. **140**, A1412 (1965).

and metal annihilation and creation operators, and U is the Coulomb repulsion integral between up- and down-spin electrons at the impurity site. The hopping integral V_{am} can be shown to be identical with the matrix element $\langle m|V_m'|a_0\rangle = V_{\alpha-m}$ used in Sec. II. Our approximation consists of neglecting magnetic effects. We thus set $U=0$, regard as superflous the impurity spin index, and introduce the subsidiary condition given by Eqs. (A2) and (A3) which guarantees a maximum electron charge of unity on the impurity. Thus Eq. (A5), in the single-electron approximation, becomes

$$H_{se}\approx \mathcal{E}_\varphi{}^a n_a+\sum_m \mathcal{E}_m n_m+\sum_m (V_{am}c_a{}^\dagger c_m+\text{H.c.}).$$

Following the standard analysis of this type of Hamiltonian,[10] the virtual-impurity-state Green's function is

$$G_{aa}(\mathcal{E})=\left(\mathcal{E}-\mathcal{E}_\varphi{}^a-\sum_m \frac{|V_{am}|^2}{\mathcal{E}-\mathcal{E}_m+is}\right)^{-1}$$

$$=[\mathcal{E}-\mathcal{E}_\varphi+i\Delta(\mathcal{E})]^{-1},$$

with

$$\Delta(\mathcal{E})=\pi\sum_m \delta(\mathcal{E}-\mathcal{E}_m)|V_{am}|^2$$

and

$$\mathcal{E}_\varphi=\mathcal{E}_\varphi{}^a+\frac{p}{\pi}\int_{-\infty}^{+\infty}\frac{\Delta(\mathcal{E}')\,d\mathcal{E}'}{\mathcal{E}-\mathcal{E}'}.$$

Proceeding as we did to obtain Eq. (A2), the impurity density of states is

$$\rho_{aa}=\frac{1}{\pi}\frac{\Delta(\mathcal{E})}{(\mathcal{E}-\mathcal{E}_\varphi)^2+\Delta^2}.$$

This expression, together with the neutrality condition, Eq. (A3), is the result of using the Anderson Hamiltonian in the single-electron approximation and is seen to be almost equivalent to the straightforward perturbation theory used in the text. The weakness of the single-electron approximation is, of course, that we have no way of dealing with magnetic effects. In this approximation there is no way of differentiating between an impurity state with one up- or down-spin electron and an impurity state with half an up spin and half a down spin. For present purposes this does not matter, although in future work we hope to clear up this approximation. We also note that this approximation is meaningful only when the impurity has no electron affinity level near the Fermi level of the metal, or, in other words, when there is a vanishingly small probability of forming a negative-ion impurity. This certainly is a valid approximation for the alkali and alkaline-earth atoms which are close to being a singly charged positive ion.

One possibly confusing detail is concerned with the fact that the lifetime factor Γ used in the text is different by a factor of 2 from Δ, the lifetime factor used in Anderson theory; that is, $\Delta=\frac{1}{2}\Gamma$. This factor-of-2 difference arises from historical reasons in which the adsorbate Γ was defined simply through a straightforward application of time-dependent perturbation theory.[4,6,7] Although this definition should not affect any of the physics, care must be taken in going from numerical results in adsorption theory to numerical results in Anderson-type theory.

Finally, we note that this whole problem could be formulated within the transfer-Hamiltonian picture. Then the theory would closely resemble the Kondo-like exchange-tunneling theory of Appelbaum.[65] However, the physical content of the theory, as relevant to resonance-tunneling spectroscopy, would probably be changed very little.

[65] J. Appelbaum, Phys. Rev. Letters 17, 91 (1966).